Review

Ultrasonically triggered drug delivery: Breaking the barrier

Ghaleb A. Husseini[a,*], William G. Pitt[b], Ana M. Martins[a]

[a] American University of Sharjah, Sharjah, United Arab Emirates [b] Brigham Young University, Provo, UT, USA

The adverse side-effects of chemotherapy can be minimized by delivering the therapeutics in time and space to only the desired target site. Ultrasound offers one fairly non-invasive method of accomplishing such precise delivery because its energy can disrupt nanosized containers that are designed to sequester the drug until the ultrasonic event. Such containers include micelles, liposomes and solid nanoparticles. Conventional micelles and liposomes are less acoustically sensitive to ultrasound because the strongest forces associated with ultrasound are generated by gas–liquid interfaces, which both of these conventional constructs lack. Acoustically activated carriers often incorporate a gas phase, either actively as preformed bubbles, or passively such as taking advantage of dissolved gasses that form bubbles upon insonation. Newer concepts include using liquids that form gas when insonated.

This review focuses on the ultrasonically activated delivery of therapeutics from micelles, liposomes and solid particles. In vitro and in vivo results are summarized and discussed. Novel structural concepts from micelles and liposomes are presented. Mechanisms of ultrasonically activated release are discussed. The future of ultrasound in drug delivery is envisioned.

1. Introduction

Nanotechnology has found increasing application in biomedicine in part because the size of the therapeutic or device matches the size of the targets, which facilitates controlled delivery in time and space. Therapeutic drugs are directed to micron-sized cells and nanosized cellular substructures such as membrane protein complexes, internal organelles, ribosomes and other control structures, chromosomes and DNA.

Targeted nanotechnology drug delivery, which is the use of nanosized drug carriers to deliver therapeutic agents to specific tissues, cells or subcellular structures, is especially important in modern medicine, as a means to deliver these compounds to their site of action, instead of indiscriminately subjecting the whole body to their action. Targeted delivery provides, for example, a way to avoid the side effects in cancer chemotherapy. In addition, the fact that specific molecular receptors are overexpressed in cancer cell membranes makes it possible to synthesize nanocarriers tagged with ligating molecules, leading to receptor-targeted chemotherapeutic technologies.

Ultrasound (US) is well known for its use in diagnostic imaging in the medical field [1]. More recently, however, US has found a niche for the treatment of several diseases such as diabetes, stroke, cancer, cardiovascular pathologies, infections, osteoporosis, thrombosis, glaucoma, nerve damage, skin wounds and bone fractures, either by itself or in combination with drugs [2].

The use of US in combination with drug delivery nanosystems has been extensively studied in the last three decades [3–17]. Although US can be used to enhance the activity of chemotherapeutic drugs in their free form (i.e., not attached to a carrier), its use in conjunction with drug delivery nanosystems has garnered ample attention in the last 20 years. This paper reviews the use of therapeutic-loaded nanocarriers in conjunction with the application of US as a controlled release trigger mechanism. A brief introduction to US will be followed by a review of its application in triggered drug delivery.

2. Ultrasound in drug delivery

2.1. The physics of ultrasound

Ultrasound is the transmission of pressure waves through a medium such as air or water at frequencies of 20 kHz or higher, frequencies above the normal range of human hearing [18]. An oscillating piezoelectric crystal is most often the source of US, and its transmission into fluid or tissue requires a medium such

as gel or water to provide contact with the piezoelectric transducer. These transducers translate an applied voltage waveform into linear motion of the transducer's face, which produce the pressure waves that are transmitted through the medium. Low frequency US refers to frequencies lower than 1 MHz, while the medium range refers to 1–5 MHz, and high frequency US is greater than 5 MHz [19]. The power carried per cross-sectional area of the ultrasonic beam, also known as the intensity or power density (W/cm^2), is another essential characteristic of medical US [18].

Unlike light waves, ultrasonic waves are a more physical phenomenon: the transmitting medium undergoes a slight oscillatory displacement due to the compression and expansion that is caused by the passing pressure waves. These are physical forces that push and stress cells and tissues; yet they usually are not themselves sufficiently strong to disrupt cell membranes, until their energy is concentrated by the presence of gas bubbles [20–22]. US also differs from light waves in the amount of absorption and scattering (collectively called attenuation) that occurs as the waves pass through the medium. Depending on the wavelength and the tissue type, US can penetrate tissue more deeply than visible light. Attenuation depends on the frequency of the waves and the nature of the medium. Water and ultrasonic gel have very little attenuation, while muscle, bone and lung tissues have high attenuation. Consequently US does not penetrate easily through bone and lung tissues. Low frequency US penetrates more easily into tissues because attenuation decreases as US frequency decreases [23].

2.2. Interactions between US and biological systems

The effects of US on biological systems are classified into the two general categories of thermal and non-thermal effects. The absorption of acoustic energy by fluids and tissues leads to thermal heating effects, as in the application of US to generate hyperthermia [20,24–29]. This can be useful in targeted drug delivery to heat the drugs, drug carriers, and/or exposed tissues [18], which increases drug release, diffusion, permeation, and cell uptake. US-generated hyperthermia can be used by itself (drug-free hyperthermia) or as an adjuvant in chemotherapy for treatment of many cancers, including breast cancer [25,26,28–30]. Furthermore, it can be used for moderate warming of tissues in physical therapy [24].

Generally, non-thermal effects are associated with cavitation, which is the formation and/or the oscillation of gas-filled bubbles in an acoustic field in response to the surrounding oscillating pressure [26]. US can excite all sizes of bubbles; however, the highest amplitude of oscillation is achieved when the natural resonant frequency of the bubbles approaches the frequency of the acoustic field. Cavitation is often categorized as inertial or non-inertial; the former leads to total collapse of the bubble whereas the latter leads only to small expansion and contraction in the size of the bubble. Non-inertial (also called stable) cavitation occurs at relatively low acoustic amplitudes where the bubbles oscillate mildly at the same frequency as the applied US waves. During this process, gas that is dissolved in the surrounding liquid diffuses to and accumulates in the bubbles, causing them to grow in size. The oscillation that occurs in non-inertial cavitation also creates a circulating fluid flow around the bubble. This flow, which is called microstreaming, has velocities and shear rates that are proportional to the amplitude of the oscillation [31–33].

On the other hand, inertial (also called collapse) cavitation occurs when larger (and often non-linear) oscillations result from an increase in the acoustic pressure or from the bubble size approaching its resonant size for the applied frequency. The total collapse of the bubble occurs as the inertia of the inward-moving water surface overcomes the internal pressure of the bubble. The extreme compression of the gas by the inward-moving water creates pressures of more than 100 atm and produces temperatures on the order of magnitude of thousands of K [34,35]. Following collapse, the rebound of expanding gas creates a shock wave. These events and the free radicals generated by the high temperatures can produce strong stresses on cells, damaging or even destroying them. Furthermore, if a bubble is near a solid surface such as large semi-rigid cell, the collapse may be asymmetrical, which ejects a liquid jet at sonic speed toward the surface [34]. If the solid surface is a blood vessel wall, skin, a large cell or a semi-rigid vesicle, the jet can pierce the surface. In the absence of a solid surface, the bubble may or may not sustain multiple collapses before fragmentation leads to smaller bubbles that serve as cavitation nuclei, that grow in size, and that eventually collapse again, thus renewing the cycle of growth and collapse [34,35].

The above-described effects are caused by collapse cavitation, and can have great impact on nearby cells; however, non-inertial (stable) cavitation may also produce significant bio-effects on the cells. At high amplitudes, the shear forces associated with noninertial cavitation are capable of shearing synthetic vesicles such as liposomes and micelles [32], shearing open red blood cells [21] or other cells, which may allow direct entry of a drug into the cytosol [21,36,37]. In addition, cavitation bubbles may increase drug interaction with the cells by up-regulating pathways related to stress response [38].

Several techniques can be used to detect cavitation, such as measuring subharmonic and ultraharmonic oscillations [39–41], noting a shift in the background of acoustic noise, trapping of free radicals, and recording sonoluminescent emissions [42]. Collapse cavitation can be implied from

measuring a decrease in acousticrelated effects as the ambient pressure is increased in experiments, since increased ambient pressure compresses the bubbles and suppresses the amplitude of oscillation [38,40–43].

There are only a few reports of non-thermal effects not associated with cavitation that are involved in the drug delivery process [44]; these primary radiation effects may include radiation pressure, radiation torque, and acoustic streaming [45,46]. However, the fluid or particle motion caused by acoustic streaming or radiation pressure may also beneficially increase convective transport of the drug toward or into cells.

2.3. The uses of ultrasound in biomedicine

Ultrasound finds very useful applications in biomedicine because of its thermal and non-thermal effects. Like optical or audio waves, ultrasonic waves can be reflected, refracted, propagated through a medium [27,34,47,48], or focused on a particular volume of tissue [22]. The technology for ultrasonic wave control and delivery is well advanced in the areas of diagnostic imaging [1] and flow measurements. Diagnostic imaging uses pulsed US at low average intensities but high pulse intensities and high frequencies. By comparison, tissue heating uses high average intensities and moderate to high frequencies, and may be delivered in continuous of pulsed waveforms. The main advantage of US in medicine is its noninvasive nature – no insertion or surgery is required. A water-based gel is applied on the skin to exclude the presence of air and then the transducer is placed in contact with the skin or tissue. This review focuses on the use of US for targeted nanoparticle-encapsulated drug delivery. Reviews of non-nanoparticles applications of US in drug delivery can be found elsewhere [2,18,49,50].

2.4. Ultrasound-triggered mechanisms of drug delivery

In ultrasonically targeted drug delivery, a careful balance in acoustic parameters is needed because the same energetic cavitational processes that actuate drug delivery may also be harmful to cells and tissues. Low intensity stable cavitation may not be sufficiently energetic to release and deliver the drug, but very high intensities may irreversibly damage tissues and cells.

Therefore, it is necessary to find a cavitation level that produces the desired effects without causing undesired damage to the cells. Firstly, there should be sufficient bubble activity to permeabilize the cell membrane without causing cytotoxic damage to the cells. Secondly, the intensity level should create an adequate number of cavitation events, such as sonic jets in blood, to promote extravasation from capillary walls without killing large numbers of endothelial cells or causing thrombosis. Furthermore, enough shear stress and microstreaming should occur to open drug-containing vesicles without lysing the cells [18]. These mechanisms are illustrated in Fig. 1.

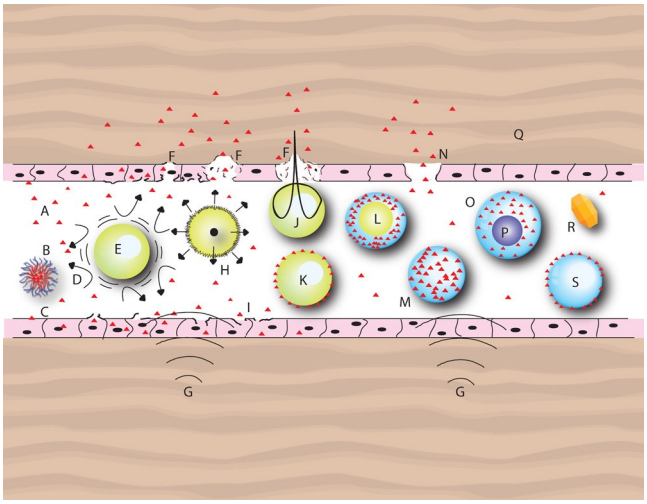

Fig. 1. Illustration of various modes of drug delivery associated with ultrasound. Gas phase is represented by yellow, aqueous phase is represented by blue, and perfluorocarbon phase represented by violet. (A) therapeutic agent (triangles); (B) drug-carrying micelle; (C) non-ruptured cells with increased membrane permeability due to insonation; (D) microstreaming around cavitating bubble; (E) gas bubble undergoing stable cavitation; (F) completely pierced and/or ruptured cells; (G) ultrasound passing through tissue; (H) collapse cavitation event emitting a shock wave; (I) cell with damaged membrane from ultrasonic events; (J) asymmetrical bubble collapse producing a liquid jet that pierces the endothelial cell; (K) microbubble decorated with therapeutic agent on its surface; (L) gas bubble inside a liposome carrying therapeutic agent in the aqueous phase; (M) standard liposome with therapeutic in the aqueous phase; (N) gap or fenestration in the endothelial lining allowing extravasation; (O) eLiposome with therapeutic in the aqueous phase; (P) perfluorocarbon droplet of the eLiposome; (Q) extravascular tissue; (R) solid nanoparticle; (S) liposome with therapeutic agent on exterior surface. (For interpretation of the references to color in this figure legend, the reader is referred to the web version of this article.) Adapted from reference [18].

The site-specificity of US-targeted drug delivery allows the localization of drug interactions to the target tissue only, and hence it treats the tumor site while sparing the rest of the body from harmful side effects. Additionally, there seems to be a synergistic effect between the pharmacological activity of some drugs and US [8,30,51–54].

Ultrasound enhances drug transport through tissues and across cell membranes by various mechanisms [18,20,55]. These mechanisms of acoustically activated drug delivery are still under investigation but appear to include: (i) enhanced convective transport; (ii) perturbation of the drug carrier; (iii) capillary rupture; and (iv) cellular membrane permeabilization [18]. These are discussed in turn below.

2.4.1. Enhanced transport

Enhanced transport derives from the oscillatory motion of the fluid that has been exposed to US and does not necessarily depend on the presence of collapse cavitation. This motion increases the transport of the free or encapsulated drug due to an increase in micro-convection which is often manifested as an increase in the effective diffusivity of molecules [56].

In the presence of oscillating bubbles, drug transport is greatly enhanced over simple diffusion. The generation of convection currents from a stable oscillating bubble involves two mechanisms: (i) microstreaming, which was defined previously; and (ii) acoustic pressure, the net force acting on suspended bodies in the proximity of an oscillating bubble, which pushes toward the bubble those bodies that are more dense than the suspending liquid and repels from the bubble those that are less dense [20]. These mechanisms lead to a series of events that eventually lead to the release of the drug. At the start of insonation, other microbubbles will be pushed away from the primary oscillating bubble, and as every bubble is a primary oscillator to all others, this tends to produce a rather uniform distribution of bubbles in the insonated fluid. On the other hand, drug carriers that are denser than the surrounding fluid, such as micelles, particles, liposomes, and eLiposomes [57–60], will be convected toward the bubble. These drug-containing vesicles are drawn into the microstreaming field adjacent to the bubble, and eventually are sheared open to release their contents [32].

2.4.2. Perturbation of the drug carrier

Ultrasound disrupts drug carriers by two general mechanisms. Firstly, as mentioned above, when acoustic pressure and velocity gradients cause shear stress that surpasses the cohesive strength of the vesicle, the latter will rupture and release its contents. Secondly, mechanisms involving collapse cavitation produce extreme stresses such as shock waves, microjets, local extreme temperatures, and damaging free radicals, all of which can disrupt carriers.

2.4.3. Cell membrane permeabilization and capillary rupture

The third major contribution of US to drug delivery relates to cellular membrane permeabilization and capillary poration that occur as a result of stress caused by cavitation events. US by itself, in the absence of bubble cavitation, has only a small effect on cells and tissues, apart from the hyperthermia that may occur for high frequencies and shear stresses at very high intensities [20,61–63]. However, cells in the proximity of cavitation events are, like vesicles, subjected to microstreaming, shock waves and sonic jets, any of which may compromise the cell membrane integrity. Blood vessel poration and rupture has been noted [64–66].

3. Drug delivery carriers designed for use with ultrasound

The simplest form of drug delivery involves the use of a free drug without a carrier system. Unless the free drug has targeting abilities, this non-targeted method affects other healthy cells and tissues in the body due to undesired interactions with the drug. On the other hand, using nanoparticle carriers such as micelles, liposomes, or solid nanoparticles prevents premature and extraneous delivery of the drug, and also allows targeting to the desired tissues. While any carrier of this type is at least somewhat useful in reducing wholebody exposure, some carriers are designed to release their cargo when activated by US. Those will be emphasized in the following sections after a general introduction to targeted drug delivery.

Nanoparticles range in size from 1 nm to 1 m. They can be classified as solids, liquids or gases depending on their physical state at room temperature. In most medical applications, the solid or liquid nanoparticles are dispersed in a liquid, forming suspensions or emulsions [67]. Combinations of gas, liquid and solid can be developed. For example, Unger et al. [54] created nanoconstructs called “lipospheres”, a hybrid between liposomes and microbubbles, and used them as carriers for the solid anticancer drug Paclitaxel. Thus gas, liquid and solid were probably present in that drug-carrying construct.

The drug can be transported either by conjugation to the carrier or by encapsulation within the carrier. In conjugation, the drug is bonded to a part of the carrier, and it can be released at the target site by the degradation of a chemical link, for example with the help of enzymes or changes in pH (see Section 4.1). However, US by itself is not sufficiently energetic to break covalent bonds. But collapse cavitation has been employed to generate free radicals that then interact with and cleave the linking bond [68].

The use of US to release encapsulated drug from liposomes or micelles is at least as common as cleaving a conjugation. Theoretically, these nanocarriers are fairly transparent to US as a stimulus unless they contain gas. However, even carefully prepared liposomes and micelles may contain dissolved gas, and the surrounding liquid may have some gas; bubbles may form and become acoustically active under high intensity insonation [69,70]. As explained previously, these vesicles in general can be drawn toward cavitating bubbles, which will shear them open.

3.1. Micelles

A micelle is a nanosized spherical vesicle with a hydrophobic core and hydrophilic corona. It forms when amphiphilic surfactant molecules are dissolved in water and aggregate together. These are often used in drug delivery as the hydrophobic center of the micelles sequesters hydrophobic drugs until the micelles is disrupted, hence minimizing the premature drug interaction with cells and tissues [63].

Some micelle surfactants are composed of a hydrophilic head and fatty acid esters that form the hydrophobic moiety. The size of the micelle is determined by the molecular size and geometry of the surfactants [71], and its structure depends on the hydrophobic/hydrophilic interactions within itself and with the environment [72].

Polymeric micelles can also be formed from polymers that have alternating hydrophilic polyethylene oxide (PEO) and hydrophobic blocks such as polypropylene oxide (PPO), polylactic acid (PLA), or other polyethers or polyesters. These copolymers may be diblock, triblock or even more complex structures [73,74]. Recognition and clearance of micelles by the reticulo-endothelial system can be avoided by inhibiting the adsorption of opsonin proteins to the micellar surface and PEO polymers reduce protein adsorption in general and opsonization in particular. Thus PEO block copolymers are useful in forming drug-delivering micelles because a hydrophobic therapeutic accumulates in the hydrophobic (PPO, PLA, etc.) core while the PEO chains extend into the aqueous solution to reduce the rate of the particle clearance [6].

The concentration at which micelles are formed is called the critical micellar concentration (CMC) [75]. The CMC of polymeric micelles is usually much lower than that of micelles formed from low molecular weight surfactants [76].

Pluronic®, a member of the poloxamer family of triblock copolymers that has a PEO_x–PPO_y–PEO_x structure, is the most common copolymer employed to form micelles that are used in acoustically activated drug delivery (e.g., P105, F127, P85, L61) [67,76–81]. The

Molecular CMC of Pluronicweight® 105 is ∼1® wt% and at the room PPO/PEO temperature block length [82].ratio The of Pluronic

as well as the concentration of the solution determine the phase state (dissolved or micellar) of the Pluronic® micelle at a given temperature [77–80]. For extravasation at the tumor site to occur, the hydrodynamic radius of these micelles should range from 5 to 20 nm at physiological temperatures. The physical and biological properties of Pluronic® compounds have also been reviewed (see [83]), especially those of P105, the most widely used copolymer for ultrasonic drug delivery [11–14,72,84–87]. Depending on the concentration of the solution, P105 exists as unimers, associates as loose aggregates or forms dense micelles. When P105 forms dense micelles [72], the core may contain a small amount of water but can still encapsulate hydrophobic and amphiphilic drugs. According to an electron paramagnetic resonance (EPR) study, this occurs at concentrations of 4 wt% or higher [81].

Other Pluronic® compounds have been investigated as drug delivery systems, but the results were less satisfactory than the ones obtained with P105: the compounds with longer PEO blocks have a CMC that is too high, and those with longer PPO blocks could not dissolve easily in water [88].

Polymeric micelles such as Pluronic® offer several advantages over other types of drug carriers [89–101]: (i) structural stability – polymeric micelles are stable at low concentrations of the copolymer, and then usually dissociate slowly at levels below their CMC, sometimes taking hours or days, while conventional micelles composed of low molecular weight surfactants typically dissociate in milliseconds [90–92,94–101]; (ii) long shelf life; (iii) stability in blood and other biological fluids: due to the presence of PEO chains in their corona, these micelles take longer to be recognized and thus cleared, hence they have a longer blood circulation time [102]; (iv) sufficiently large size (15–30 nm) that excludes them from renal excretion; (v) sufficiently small size to allow extravasation at the tumor site which allows them to penetrate into the leaky tumor capillaries; (vi) PPO core that is sufficiently hydrophobic to stabilize the micelle and sequester hydrophobic drugs [85]; (vii) simplicity in drug incorporation – hydrophobic drugs can be easily incorporated just by mixing – when compared to the covalent bonding of the drug to polymeric carriers [86,103]. In addition, Pluronic® surfactants have gained special attention since they were shown to sensitize multidrug resistant (MDR) cancer cell lines even at low concentrations [104–106] (see Section 4.1), and because they have low in vivo toxicity [105].

In addition to passive targeting based on size, micelles can be modified with ligand moieties, such as antibodies, oligosaccharides, peptides and more, which are attached to the hydrophilic shell-forming blocks [107]. This leads to ligand targeting since it allows the micelles to specifically bind to antigens or receptors that are overexpressed on the surface of tumor cells [75]. Kabanov and co-workers [108] were one of the first to report the incorporation of brain-specific polyclonal antibodies into haloperidol-containing Pluronic® P85 micelles, as a way to improve the delivery of this drug to the brain of mice (by penetrating the blood brain barriers). Several reports concerning the use of monoclonal antibodies as targeting moieties have also been described [75,109,110]. Another extremely important and widely used ligand is folate, since the folate receptor is overexpressed in many types of cancer cells in response to the increased folate requirement for

biosynthesis of nucleotide bases [111]. Other ligands have been studied and are reviewed elsewhere [75,109,110].

Currently, the most promising micelle-based anticancer therapies rely on multifunctional micelles that combine targeting ligands and triggered release [75]. The triggered release of drugs can be achieved by using stimuli-responsive micelles that release their drug load only in response to environmental or physical stimuli, such as the lower pH in tumor tissue, heat, sound, or light. An excellent review is available [112].

Several reports have described the combination of ligand targeting with pH sensitivity as a triggered release mechanism [113–117]. These studies have shown that the combination of ligand targeting with triggered release resulted in increased cytotoxicity and antitumor activity. The combination of actively (ligand) targeting polymeric micelles and applying US as external stimulus was recently described by Husseini and co-workers [118] (see Section 4.2.1).

To summarize, the use of micelles in drug delivery has been commonly encountered throughout pharmaceutical history [67]. However, the combination of US and micellar carriers has only recently been studied and used as an efficient drug delivery system [119] (see Section 4).

3.2. Liposomes and eLiposomes

Liposomes are bilayered vesicles in which an aqueous core is enclosed by one or more membranous lipid bilayers mainly composed of natural or synthetic phospholipids (in many cases phosphatidylcholines) [120,121]. Liposomes can have one or more phospholipid bilayers and they are characterized in terms of size, surface charge and bilayer number [120]. The bilayer is a potential site for lipophilic drugs whereas hydrophilic drugs are solubilized in the aqueous core [122]. A challenge of delivering hydrophobic pharmaceutics is that they may destabilize the bilayer and make the liposome fragile.

The sizes of liposomes range from 25 nm to 25 m in diameter, much larger than polymeric micelles (5–30 nm) [18].

Microbubbles and nanobubbles are distinguished from liposomes in that they contain gas and in general are stabilized by a single layer of surfactant at the liquid/gas interface [18].

Lipids that form liposomes usually aggregate spontaneously to form multilamellar vesicles (MLV) when placed in an aqueous solution at a concentration higher than the critical aggregation concentration (CAC), and at a temperature above the solid-ordered (SO) to liquid-disordered (LD) phase transition [123,124]. The size of MLV can be decreased by the use of high-intensity low-frequency US [125–127], freeze–thaw or extrusion [128]. These processes often reduce MLV to unilamellar (only 1 bilayer) liposomes.

The lipid bilayers of most phospholipids have a phase transition from the SO to the LD (and vice versa) that occurs at a temperature which is dependent on the molecular structure of the phospholipids. The LO (liquid-ordered) phase is an intermediate phase between the SO and LD phases that occurs only when cholesterol, or another membrane-active sterol, is present in the bilayer [130]. Liposomes in the LD phase are more permeable than liposomes in the LO and SO phases. Liposomes undergoing phase transition are even more permeable due to defects in the bilayer packing, related to the existence of SO and LD regions [131].

This temperature-dependent phase transition was first explored by Yatvin and co-workers, who presented the idea of thermal control of drug delivery using temperature-sensitive liposomes (TSL) [132]. The lipid composition of the liposomes determines their thermotropic behavior, which is the change in orientation based on the local temperature. Hence, temperature affects their permeability, the stability of drug loading, and the rate of drug release [133]. Several reports have been presented concerning the use of hyperthermia and temperature-sensitive liposomes in drug release strategies. A recent review is available [134].

It was also observed that during the SO to LD phase transition there is increased absorbance of ultrasonic energy by the liposomal lipid bilayer [129]. In fact, ultrasonic waves can be used to induce both thermal and non-thermal effects in liposome carriers (see Section 5). However, liposomes in general are rather transparent to US and are not easily activated by US unless they contain gas. Hence, echogenic liposomes, bubble liposomes, acoustically active liposomes (AAL) and other constructs were designed to contain a gas phase such that they respond to US and can be used more readily as drug-delivery systems [59]. More recently, a new type of echogenic liposomes called eLiposomes, containing a phase-changing liquid emulsion droplet, has been developed in which US changes the droplet phase from liquid to gas [57–60].

The use of US to control the release of drugs from liposomes and eLiposomes, either by inducing thermal or non-thermal effects, will be discussed in Section 5.

3.3. Solid nanoparticles

Solid nanoparticles have a solid core, or at least, the material in the core forms a macroscopic solid at room temperature. Unlike micelles, they are not necessarily spherical, but may be angular, especially if they consist of crystals of a protein or other therapeutic agents. In order to prevent flocculation, a surfactant is often required to stabilize a nanoparticle suspension.

There are several categories of solid nanoparticles used in drug delivery [121] generally divided into polymeric or non-polymeric. Polymeric nanoparticles are often composed of biodegradable polymers; the drug is released by erosion or degradation of the polymers, by diffusion of the drug from the intact polymeric core, or by a combination of both. In some formulations, a nanoparticle is formed by the labile attachment of the drug or prodrug to an insoluble polymer. If the polymers with the attached drugs are soluble, hydrogel nanoparticles can be formed by physically or covalently crosslinking the polymer once the nanoparticle has been formed, so that it will swell but not dissolve in the fluid. One example is a dendrimer, a highly branched nanosized hydrophilic polymeric drug carrier [135]. Drugs can be attached to the ends of the branched polymer arms or small drugs can be sequestered inside the dendrimer and then released by diffusion.

One of the most widely studied families of solid nanocarriers for drug delivery are the ring opening polyesters, which include poly(caprolactone) (PCL), poly(lactic acid) (PLA), poly(glycolic acid) (PGA) and poly(lactic-co-glycolic acid) (PGLA) [136]. Several of these nanoparticles are approved by the USA Food and Drug Administration (FDA) for drug delivery and diagnostics in cancer, cardiovascular disease, and have also been used in vaccines and tissue engineering [137,138].

Non-polymeric nanoparticles include solid aggregates of hydrophobic proteins or drugs that may partially or completely crystallize, mesoporous silica containing voids that can be filled with drug, and nanotubes and fullerenes which are hollow rods and spherical cages of graphitic carbon that can carry drugs within their volume or attached to their surface [139].

Solid lipid nanoparticles consist of a solid lipid core that can carry a hydrophobic drug, which is often stabilized by an external monolayer of charged surfactant. Nucleic acid nanoparticles are closely related and consist of negatively charged DNA or RNA polynucleotides that condense with cationic lipids or polymers. Once the charge is neutralized, the complex is usually hydrophobic enough to form nanoparticles that may enter the cell by endocytosis or pinocytosis [140]. Additionally, noble metal nanoparticles have also been used as drug delivery vehicles [141,142].

4. Micelles and ultrasound

4.1. Micellar drug carriers (stabilized vs non-stabilized)

As mentioned previously, micelles are aggregates of amphiphilic molecules that spontaneously arrange (in water) to have a hydrophobic interior volume and a hydrophilic exterior. While micelles were traditionally made from small surfactant molecules, polymeric micelles have come into use in drug delivery systems (see Section 3.1) since they offer several advantages over other types of micelles. These include slower dissolution rates, a large hydrophobic core volume, and the ability of investigators to tailor the hydrophobic/hydrophilic balance in the micelle core to optimally match the payload molecule. Ample literature exists on the use of polymeric micelles as drug delivery carriers [11,12,46,81,84,88,90,96,98–103,143–149]. In this section we will focus on polymeric micelles, especially on the Pluronic® family of micelles.

Drugs can be loaded into micelles by physical association using processes as simple as mixing the drug with the micelle suspension. Several anticancer drugs, such as doxorubicin (Dox), ruboxyl (Rb) and Paclitaxel, have been physically entrapped in polymeric micelles [86,150–152]. The encapsulated drugs are then released at the target site.

Alternatively, chemical conjugation may be used to incorporate drugs into micelles, with drug attachment to either the core or the shell. A common example is covalently linking the drug to the hydrophobic block of the copolymers, yielding micelles of block copolymer–drug conjugates [90,98,101,153]. Using this method, Yokoyama and co-workers studied the formation of a drug-block copolymer conjugate (adriamycin-conjugated poly(ethylene glycol)-poly(aspartic acid) block copolymer) [101].

As mentioned, Pluronic® micelles are commonly used in drug delivery. These are a family of PEO–PPO–PEO copolymers, which became popular because they also counteract resistance mechanisms in MDR-cells [143]. The micellar nature of the Pluronic® copolymer enables hydrophobic drugs to be accumulated in the hydrophobic core, thus protecting the surrounding healthy cells from unintended release of free drug. Pluronic micelles can exist in various physical forms, depending on the local concentration and temperature. For example, P105 can exist as micelles (5–25 nm) and at concentrations higher than 4 wt% it can also exist as dense aggregates; these nanoparticles encapsulate hydrophobic drugs in their PPO core [81]. At the same time, proteins are prevented from adsorbing to the micellar surface due to the corona of the hydrophilic PEO chains, which increases the circulation time of the carriers. These systems are commonly used in ultrasonic drug delivery (see Section 4.2).

The effect of Pluronic® compounds in overcoming resistance mechanisms in MDR-cells has been widely studied. A good review is found in [154]. The mechanism of sensitization of the MDR cell lines by Pluronic® compounds seems to involve a selective decrease in the ATP levels in MDR cells [155]. Alakhov and coworkers investigated the hypersensitization effect of the Pluronic® P85 block copolymer on MDR-human ovarian carcinoma cell lines, and observed a substantial increase in the cytotoxic activity of Daunorubicin (an analog of Dox) and other MDR-type drugs, in the presence of 0.01–1 wt% copolymer

[104]. A 290-fold and 700-fold increase in sensitivity was observed in MDR CHRC5 Chinese hamster ovarian cells and MCF-7/ADR human breast carcinoma cells, respectively, when Venne and co-workers studied the cytotoxic action of Dox in the presence of Pluronic® L61 [106]. Batrakova and co-workers have studied the effects of epirubicin (EPI) and Dox in micelles of Pluronic® L61, P85 and F108 in MDR-cancer cell lines, and showed that their anti-tumor activity was higher than that of the free drugs [143]. Additionally, they observed that higher concentrations (above the CMC) of the surface-active triblock copolymer resulted in less accumulation of Dox inside the cellular compartment, discovering serendipitously that the antineoplastic drug was sequestered inside the hydrophobic core of the resulting micellar solution. An equilibrium distribution is established between unimers and micelles at concentrations higher than the CMC. Despite the ability of unimers to overcome the MDR behavior, only the micelles are observed to protect the healthy cells by sequestering drug. Some block copolymers may be harmful at such high concentrations; therefore, it is necessary to always include suitable controls in all the in vitro experiments. A recent paper by Hong and co-workers [156] addresses the successful delivery of Pluronic® P85 unimers to MDR cells using pH-sensitive mixed micelles.

Other types of polymeric micelles have also been studied. For example, Kwon and co-workers, investigated the entrapment of Dox in micelles of poly(ethylene oxide)–poly(-benzyl-laspartate) (PEO–PBLA) [96]. Their results showed that Dox was stably entrapped in the micelles and its pharmacokinetics was markedly modified.

Using a more complex block copolymer of poly(Nisopropylacrylamide-b-butylmethacrylate) (PIPAAm-PBMA), Chung and co-workers [89] developed micelles that respond to thermal stimulus. The micelle's inner core was formed from aggregates of PMBA segments and the outer shell PIPAAm chains played a role in the stabilization of these micelles as well as the initiation of the thermo-response. Dox was successfully loaded into the core of the micelles and the drug could be released due to reversible structural changes in the micelles upon heating and cooling.

The main challenge when using Pluronic® P105 and other polymeric micelles to deliver chemotherapy drugs is that they are not stable enough to be used in vivo because they may be diluted below their CMC when injected into the blood stream, which may dissolve the micelle and prematurely release the drug [18]. The polymer concentration should be higher than the CMC to prevent premature dissolving of the micelle and release of the drug before reaching the target site. However such high concentrations of the polymer may be intolerable to the body [19]. There are several ways to overcome this disadvantage.

A more stable micellar drug carrier, NanoDeliv™, is synthesized from P105 by copolymerizing an interpenetrating network (IPN) of thermally responsive acrylates in the hydrophobic core [88]. After accumulation of the drug in the hydrophobic core due to expansion of the thermally responsive network at relatively cool room temperature, the warming of NanoDeliv™ upon injection into the body causes the contraction of the network, and this further traps the drug molecules and Pluronic chains in the micelles. Upon injection and dilution, the IPN prevents the degradation of the micelles and keeps the drug associated with the core, minimizing premature release. As the temperature increases, the association of water with the PEO blocks decreases and the micelle shrinks [88]. The in vitro half-life of these stabilized micelles is about 17h. NanoDeliv™ micelles have been shown to release

Dox upon insonation, but release smaller quantities of drug for the same US intensities [157]. The size of Nanodeliv™ micelles

(∼60 nm at 37 ◦C) is optimal for them to pass through capillaries and be extravasated at the tumor site, and yet avoid renal excretion [72].

In another example, Gao and et al. describe the stabilization of Pluronic® P105 micelles by the introduction of a PEG-diacylphospholipid, such as 1,2-distearoyl-sn-glycero-3phosphoethanolamine-N-[methoxy-(polyethylene glycol)-2000] in a 1:1 ratio [158,159]. This combination decreased the CMC and stabilized the micelles.

A family of micellar drug carriers with time-controlled degradation was also developed [148,149] and shown to release Dox upon insonation in vitro. The polymers used were PEO, N-isopropyl acrylamide (NIPAAm) and polylactate ester of hydroxyethyl methacrylate (HEMA-lactate). The main advantage of this carrier is that the lifetime and degradability of the NIPAAmHEMA-lactate block can be controlled by choosing the appropriate composition of the polymeric blocks. This micelle also released Dox upon the application of 70-kHz US [147].

Recently, drug delivery using targeting moieties has been investigated, as mentioned. The objective is, again, to minimize the unwanted side effects of drugs by reducing premature release while maximizing their concentration at the target site by ligand–receptor interactions. This technique makes use of the fact that certain membrane receptors are overexpressed in cancer cells [160–162]. The combination of receptor-targeted chemotherapy with nanoparticle drug carriers and physical stimulus (e.g., heat, US, pH change) to trigger drug release is extremely promising in chemotherapeutics.

4.2. Ultrasonic drug delivery from micelles

Unfortunately the organic molecules and polymers used to construct micelles are fairly transparent to US. Thus, direct interaction with soluble molecules is negligible, and interaction with a micelle (in the absence of a bubble) may be limited to a small amount of radiation force generated by the small mismatch in speeds of sound between water and the micelle material. These small forces are not considered strong enough to break apart micelles.

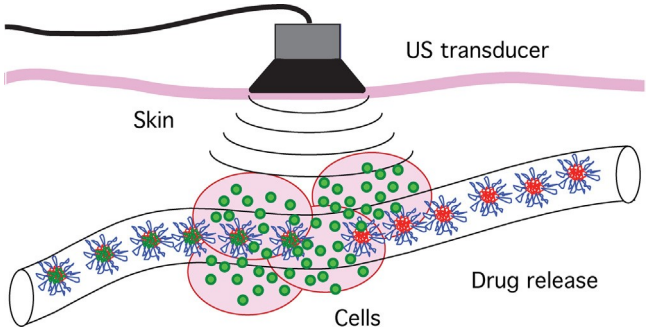

Fig. 2. Acoustically activated drug delivery from Pluronic P105 micelles. The green dots are drug molecules to be released at the targeted site. (For interpretation of the references to color in this figure legend, the reader is referred to the web version of this article.)

However, the observation that drug release from micelles has a threshold value and correlates with collapse cavitation implicates the participation of cavitating gas bubbles. Even in the absence of added "preformed" gas bubbles (such as contrast agents), it is not surprising that gas bubbles exist, since in real experiments many liquids contain dissolved gas that may nucleate into bubbles upon insonation. Furthermore, the same amphiphilic molecules that form the micelles may also stabilize the existence or promote the formation of gas bubbles. In fact the hydrophobic core of micelles may actually be a reservoir of dissolved gas molecules. For example, the solubility of nitrogen in water at 25◦C and 1 atm is 1.18 × 10−3mole%, while the solubility of N2in n-hexane at the same temperature and pressure is 1.39 × 10−1mole%, two orders of magnitude greater [163]. The hydrophobic core of micelles maybe scavengers and collectors of dissolved gas that might contribute to the formation of gas bubbles upon insonation.

Whatever the source of gas bubbles in experimental situations, the Pluronic® P105-type micellar carriers have been found to be ideal for US-activated drug release since the micelles can be perturbed by low frequency US to release the drug [12], and the drug is quickly re-encapsulated in the carrier when insonation is stopped [157]. Fig. 2 depicts the use of US and micelles to release chemotherapeutic agent at the tumor sites.

The next sections of this review summarizes the in vitro and in vivo studies that have been done using these micelles as drug delivery carriers in conjunction with US, and additionally discusses the mechanisms that have been proposed for this US-induced drug delivery.

4.2.1. In vitro results

A specially designed ultrasonic exposure chamber that measures real-time fluorescence was built to determine the drug release from Pluronic® P105 micelles under the influence of continuous wave (CW) or pulsed US [74]. The fluorescence inside the hydrophobic core of the micelle is higher than that in the aqueous environment and this enabled quantitation of the drug release through fluorescence quenching measurements. Fig. 3 illustrates the ultrasonic exposure chamber used to measure release and release kinetics of Dox from polymeric micelles.

In one of the first studies, the release of two fluorescent drugs – doxorubicin and ruboxyl – was studied using the above mentioned device, and the amount of drug release was measured in the low frequency range of 20–90 kHz CW and pulsed US [12]. It was observed that the drug release was higher when 20 kHz US was applied. The release deceased with increasing US frequencies despite higher power densities, suggesting that cavitation played an essential role in the release of the drug. The original hypothesis was that stable cavitation was responsible for the drug release from stabilized and non-stabilized micelles. However, subsequent experiments carried out using a modified version of the ultrasonic exposure chamber mentioned above, showed a correlation of drug release with subharmonic emissions and a sudden appearance of a broadband noise background attributed to white noise from shock waves, characteristic of collapse cavitation [46].

Further studies carried out at 70-kHz indicated that the intensity threshold requirement to release the drug (Dox) ranged from 0.35 to 0.4W/cm^2 [136]. At this intensity, sub-harmonic emissions and broadband noise were observed which reflected the occurrence of inertial cavitation [139]. The data was further corroborated by electron paramagnetic resonance (EPR) spectroscopy using 5,5′dimethyl-1-pyrroline-N-oxide (DMPO) as a radical trap [12]. The US intensity at the onset of drug release coincided with the formation of DMPO-OH adducts formed by trapping of OH radicals with DMPO. The OH radicals were generated by the extreme temperatures inside the collapsing bubbles during the insonation of a 10 wt% P105 micellar

solution. The authors hypothesized that shock waves caused by the collapse of cavitating bubbles were responsible for the perturbation of the micellar structure that caused the drug release.

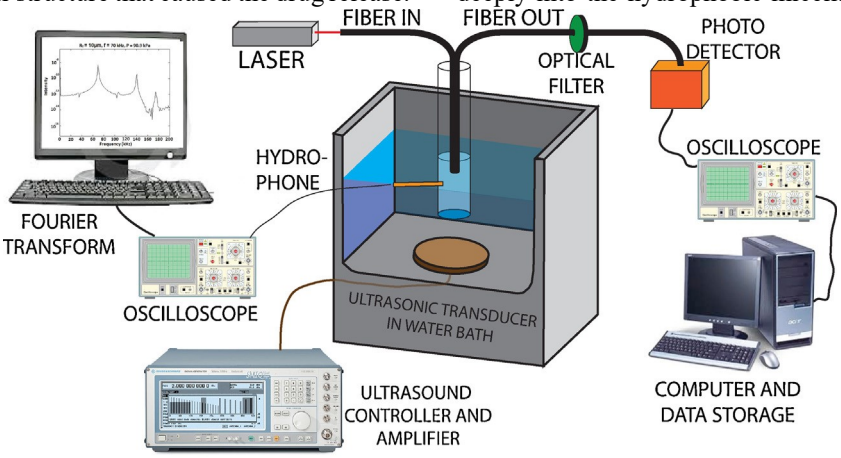

Fig. 3. The ultrasonic exposure chamber with fluorescence detection used to measure the release of Dox from polymeric micelles. The chamber employed an argon ion laser where the laser beam was directed to a beam splitter attenuator. Drug concentration was quantified by measuring the fluorescence emissions produced by an excitation wavelength of 488 nm. A fiber optic probe was used to collect fluorescence emissions. The emitted light was directed through a multinode dielectric band and filter to a silicon detector. The filter was used to cut off any emissions with a wavelength below 535 nm. The detector signal was digitized with an A/D converter and sent to a computer for storage and processing. Acoustic spectra were Fourier transformed to determine bubble cavitation activity.

Inertial cavitation occurred at both 70 and 476 kHz; however, this did not necessarily lead to the release of Dox from Pluronic® micelles since it was observed in the research that no release occurred at 476 kHz [136]. In further studies, the Keller–Miksis–Parlitz equation was used to model the bubble oscillation behavior at both frequencies to determine the differences between bubble cavitation [164]. At 70 kHz, the bubble was shown to jump to chaotic behavior at a mechanical index (MI) of 0.35, whereas at 476 kHz, the bubble demonstrated a more gradual "period-doubling" route to chaotic oscillation over an MI range of 0.28–0.41 [136]. "Mechanical index" (MI), is a measure of the probability of collapse cavitation occurring.

The MI is defined as:

$$\mathrm{MI} = \frac{P^{-}(\mathrm{MPa})}{\sqrt{f\,(\mathrm{MHz})}}$$

where P− is the peak negative pressure amplitude and f is the applied frequency. Subsequent studies using a similar modeling approach compared microbubble cavitation at 476 kHz and 70 kHz and the results showed that, at 70 kHz, the bubble follows an intermittent route to chaos, which is associated with the drug release observed experimentally [165,166].

The first evidence that the drug release increased with a decrease in Pluronic® concentrations was provided in a study carried out by Husseini et al. [12]. In this study, it was also shown that the drug release decreased when the drug was inserted deeply into the hydrophobic micellar core. Additionally, it was observed that the drugs were re-encapsulated within the micelle between short pulses of US.

To study the kinetics of release and re-encapsulation of Dox from Pluronic® P105 micelles, the previously described fluorescence detection exposure chamber was used, and the results revealed the existence of a time threshold of 0.1 s, below which no significant drug release occurred, while the re-encapsulation required at least a US "off" phase of 0.1 s [84]. Maximum release occurred ~0.6 s after initiation of US and re-encapsulation commenced upon cessation of insonation. This report suggested that when insonation ceases, the drug is re-encapsulated inside the micelle. The encapsulation was a huge advantage of this system because during in vivo insonation, once the micelle and the drug leave the insonated area, the drug will be re-encapsulated back into the micellar carrier and will not affect the healthy cells downstream of the insonated area.

Long pulses of US produced drug release (and re-encapsulation) for both the stabilized and unstabilized P105 micelles. The kinetic data collected could then be described by mechanistic models that enable further understanding of the US-induced release of Dox from micelles. Dox release studied using simple models was shown to be zero-order with respect to the encapsulated drug concentration. Similarly, the re-encapsulation was shown to be first-order with respect to released Dox concentration [75]. Subsequently the data set was expanded to include new results obtained with an expanded range of operating conditions: power density, frequency, Pluronic®

P105 concentrations, and temperature. Artificial neural network (ANN) deterministic models [145] and chemical kinetic mechanistic models [167] were used to analyze the release and re-encapsulation of the drug as a function of the aforementioned variables. The modeling results showed that the drug release efficiency was inversely proportional to frequencies and directly proportional to the power density. Additionally, sensitivity plots revealed that at 20 kHz, the power density threshold for drug release was 0.015W/cm^2 at MI=0.15 and that at

70kHz it was 0.38W/cm^2 at MI=0.40. This data further emphasizes the importance of inertial cavitation in acoustically activated drug release from polymeric micelles [145]. The kinetic model built by Stevenson-Abouelnasr and co-workers [167] was further used to represent the acoustic release and re-encapsulation kinetics of Pluronic® P105 micelles at various power densities and temperatures (25 ◦C, 37 ◦C, 56 ◦C), using 70-kHz US [168]. The results showed that the residual activation energy for the micelle destruction decreased with increasing US intensity, and that higher temperatures promoted micelle destruction and delayed micelle re-formation.

Subsequently, another ANN model was built to predict the dynamic release of Dox from Pluronic® P105 micelles using 20kHz US at different power densities, with the aim to design model predictive controllers [169,170].

As mentioned previously, the rate constant of Dox release also depends on the stabilization (cross-linking) of the micelles. The in vitro release of Dox from several carriers, non-stabilized and stabilized, was investigated using the fluorescence detection chamber described previously [147]. The results showed that 70-kHz US causes more release of Dox from non-stabilized Pluronic® micelles (∼10%) than from stabilized systems such as NanoDeliv™ (∼3%).

Although 3% seems like a low amount of release, the use of pulsed US that releases small quantities with every application could theoretically release the entire drug load in the presence of cells that compete for the released Dox. A recent study also showed that the release rates of stabilized micelles are significantly lower than that of non-stabilized ones [146]. Although US appears to disturb the IPN of stabilized micelles, the time constant of the degradation is very long compared to that of the drug release from the micelles, and no significant difference was observed between the network degradation after 1 h of insonation at 70 and 476 kHz [15].

Recently, Husseini and co-workers have described for the first time, a system combining ligand targeting of polymeric micelles and US as a drug release trigger [118] (see Section 4.2.1). They synthesized Pluronic® P105 micelles with a folate targeting moiety, and studied the effect of US frequency on the release of Dox. They observed that the drug was released above a low power density threshold of 0.55W/cm^2, which confirmed that cavitation plays an important role in release from this carrier as well. The results also showed that the amount of drug released increased with the US power density, up to a maximum of 14% release at 5.4W/cm^2.

In vitro studies using cell lines and in vivo studies will be necessary to further evaluate this combination as an efficient drug delivery system to be used in anti-cancer therapy.

All of the results described previously were obtained using Pluronic® compounds as micellar building blocks. However, other types of polymeric micelles have also been studied, as shown in the following examples. Zhang and co-workers synthesized the block copolymer PLA-b-PEG, which self-assembles into spherical micelles in aqueous solution [171]. They used high intensity focused US (HIFU) to control the release of Nile Red and proposed an irreversible mechanism triggered by the inertial cavitation in the HIFU focal spot. The same group reported the disruption of micelles of poly(ethylene oxide) and poly(2-tetrahydropyranyl methacrylate) (PEO-b-PTHPMA) in aqueous solution by HIFU (1.1 MHz) [172]. The proposed mechanism was the HIFU-induced hydrolysis reaction of THPMA at room temperature, resulting in the cleavage of 2-tetrahydropyranyl groups.

4.2.2. In vitro drug delivery to cells

After studies on US-activated drug release from micelles were complete, the research moved to in vitro cell systems. Munshi and co-workers carried out a study on the use of insonated P105 micelles to deliver therapeutic to cancer cells in vitro. These studies showed that the drug's IC_{50} decreases from 2.35 to 0.19 g/ml when US and Pluronic® P105-encapsulated Dox are used synergistically [85]. Later, the same group studied the effect of exposing HL-60 cells to Dox and Dox encapsulated in either Pluronic® micelles or NanoDeliv™ [11,72,173,174]. The cytotoxicity induced by Pluronic® P105-encapsulated Dox on HL-60 cells was compared in the presence and the absence of continuous 70-kHz US [11]. The results of cell viability presented a significant synergism between US, Dox and Pluronic® micelles. In the absence of US, cells were protected from Dox by the Pluronic® (Dox at a concentration of 10 g/ml encapsulated inside P105 micelles for up to 9 h of incubation); therefore US was acting as a trigger to increase the rate of cell killing [72]. Subsequently, the comet assay was used to study the amount of DNA damage and showed that the primary mechanism of cell death was apoptosis. These results provide evidence that at these levels of insonation, gradual DNA fragmentation occurred and not necrosis [173]. Similar results were obtained when using the NanoDeliv™ micelles with Dox [174].

The uptake of Dox by cancer cells in vitro has been widely studied, using direct and indirect methods [13,86,175,176]. Indirect methods rely on the measurement of the drug depletion from the incubating medium, with the help of a spectrofluorometer. Direct methods measure the fluorescence of Dox in cells lysed in 2% sodium dodecyl sulfate (SDS) and allowed the quantification of Dox uptake kinetics and isotherms in several studies [13,86,175]. The quantification was done using flow cytometry and fluorescence microscopy. Dox is ideal for this kind of experiments due to its fluorescence. Additionally, these techniques allow the study of the drug distribution inside the cells.

Similar cytotoxic results were demonstrated using pulsed 70kHz US to study the uptake of Dox by HL-60 cells. It was observed that, for a constant "inter-burst" (US off) period ranging from 0.1 to 2 s and with a constant total insonation time, the drug uptake by the cells was higher when the insonation (US on) period was extended from a 0.1 to 2 s [176]. The amount of drug uptake, however, did not depend on the length of the "inter-burst" period, suggesting that in the presence of cells, little if any Dox is reincorporated in the micelles, indicating that the cells are very effective at competing with the micelles for the drug [175]. The same study showed that 90% of full uptake was reached in about 2.5 s of insonation, which is slightly lower, but from the same order of magnitude, as the rate of release of the drug from the micelles [72].

The effect of Pluronic® concentration on the uptake of Dox by A2780 drug sensitive and A2780/ADR MDR drug resistant ovarian carcinoma cell lines was also studied [177]. Insonation had a positive effect on drug uptake in both cell lines; however, the uptake of Dox by the cells was lower in a more concentrated Pluronic® solution (10 wt%) than in a 0.1 wt% solution [14]. The same study used confocal microscopy to show the different distributions of Dox inside the cell, with Dox being predominantly in the nucleus [177].

Pluronic® P105 was labeled with 5,6-carboxy-2–7dichlorofluorescein, a pH-sensitive fluorescence detector, which exhibits higher brightness at pH 7.4 than at the acidic pH of lysosomes or endosomes [14]. HL-60 cells were then exposed to this labeled Pluronic® P105 with and without US. In both cases, the cells took up the label and were studied by confocal microscopy and flow cytometry. The results showed a distribution of the labeled Pluronic® P105 to the membrane, vesicles and the cytosol.

The same group also studied the effect of US in the rate of endocytosis of micelles into HL-60 cells [178], using Pluronic® P105 labeled with Lysosensor Green, which fluoresces more strongly at the acidic pH (~4.8) of lysosomes and endosomes, than at the external pH of 7.1 [179]. Flow cytometry analysis of cells insonated for 1 h at 70 kHz and those of non-insonated cells were not significantly different. The fluorescent probe did not move toward a more acidic pH in the presence of US; this observation suggested that the labeled Pluronic® P105 remained outside endosomes and lysosomes. Therefore, enhancement of endocytosis might be discounted as a mechanism involved in US-assisted drug delivery. However, a later study by Rapoport et al. [119], provided evidence that acoustic stimulus enhanced the rate of endocytosis of micelles by human cell lines. Pinocytosis in the endothelial cells lining brain arterioles and capillaries can be enhanced by US as shown by Sheikov and co-workers [180]. More recently, the upregulation of endocytosis by US in endothelial cells was shown in a study of microbubble-targeted delivery [181] and a US-enhanced endocytic activity was also reported in human fibroblasts, with no US-induced structural membrane damage [182].

Different drugs and/or different micellar systems have been studied in vitro, in addition to Dox in Pluronic® and NanoDeliv™ micelles.

Tachibana et al. [8] reported an increase in HL-60 cell death under exposure to low intensity (48-kHz) US when treated with the chemotherapy agent cytosine arabinoside. Hyperthermia as a cause was ruled out since the increase in temperature did not exceed 0.2 ◦C. The insonated cells were analyzed by scanning electron microscopy, which revealed a decreased number of microvilli and a disrupted cell membrane. It was concluded that insonation disturbed and modified the cell membrane, and that this was responsible for an increased drug uptake. Several other studies showed similar evidence of cellular membrane sonoporation [183–186].

Stringham and co-workers pressurized an acoustic chamber to suppress the effects of collapse cavitation and study its role in micellar delivery of the drug calcein to colon cancer cells [187]. A series of effects result from an increase in the ambient pressure at constant US intensity: there is a decrease in cavitational activity, which appears as a reduction in the height of the subharmonic and ultraharmonic peaks in the acoustic spectrum, and this leads to a reduction in the shear stress [188,189]. Stringham's study using rat colon cancer cells showed that, in vitro, a reduction in shear stress at constant pressurization leads to a decrease in the uptake of calcein. Calcein, which normally does not penetrate the membrane of healthy cells, accumulated inside the cells during ultrasonic exposure at 476 kHz; however this accumulation decreased as the chamber pressure increased (up to 3 atm), supporting the hypothesis that inertial cavitation is directly linked to the drug uptake by the cells.

Howard and co-workers [150] studied the effect of methylcapped poly(ethylene oxide)-co-poly-(l-lactide)-tocopherol micelles and US on a breast cancer drug-resistant cell line. Without insonation, the accumulation of Paclitaxel inside the cells was less when using polymeric micelles compared to the free drug, thus confirming that using chemotherapeutic agents with the aid of nanoparticles is important for cell protection. When US was applied at 1MHz and 1.7W/cm^2 and a duty cycle of 33%, the accumulation of encapsulated Paclitaxel dramatically increased. However, they did not prove or hypothesize an uptake mechanism. Nevertheless, the combination of polymeric micelle-encapsulated Paclitaxel and US is effective in complete tumor regression in nu/nu mice that have been injected with the drug resistant tumor cell line.

A more recent study used Dox encapsulated in P105 micelles stabilized with disteroyl-phosphoethanolamine-PEG200, instead of an IPN [190]. Encapsulation of Dox in this mixed micelle reduced Dox uptake by MDA-MB-231 breast cancer cells in vitro. Application of 20-kHz US at 100W/cm^2 for 5s released about 10% of the Dox from the micelles and increased the cellular uptake, but destroyed HL-60 cells when applied for more than 5 s.

Recently, Chen and co-workers [191] developed a new polymeric P105/F127 mixed micelle and studied its effect on the delivery of the poorly soluble antitumor drug docetaxel (DTX) against Taxol-resistant non-small cell lung cancer. Their study showed that the DTX-loaded P105/F127 micelles had a higher hypersensitizing effect in the A549/Taxol cell lines.

The above-mentioned in vitro studies provide evidence that ultrasonic cavitation produces stress in the cell membrane that allows an increased drug uptake than would occur without US. This data, coupled with the finding that US creates repairable holes in cell membranes, shows a synergistic effect between chemotherapy and US in vitro: US both releases drug from nanocarriers and creates transient membrane holes through which released drug or even micelles, can enter the cytosol, thus bypassing the endocytotic pathway (see Section 4.2.4).

4.2.3. In vivo and pre-clinical results

After the understanding of the mechanism of ultrasonically actuated drug release to cells in vitro, several in vivo studies followed [87]. The most widely used model for in vivo studies is that of tumor bearing rats and mice: the Rapoport [159,192,193] and Myhr [194] groups used mice models, while the Pitt group used a rat model [195–197] to study the delivery of Dox from stabilized micelles to solid tumors.

We should first note that even in the absence of micelles, in vivo studies have revealed a synergistic effect between chemotherapy drugs and US. Several studies have shown a decrease in tumor growth simply by exposure to US and free drug [198].

In an early in vivo study, the Pitt group used a rat model to study the effect of Dox on a colon carcinogen cell line DHD/K12/TRb inoculated in each upper hind leg with a subcutaneous injection [195,196]. Power density (1 and 2W/cm^2), ultrasonic frequency (20 and 70 kHz), Dox concentration (1.33, 2.67, and 8 mg/kg), power train (continuous and pulsed), and treatment regimen (once and twice weekly) were variables implemented in the abovementioned experiments. Free or NanoDeliv^{TM}-encapsulated Dox was systemically injected (via tail vein) to allow for equivalent exposure to each tumor in each leg; the US was applied for 1 h every week for an entire month to only one tumor on one leg of the rat. By carrying out a paired statistical analysis to investigate the effect of insonation on tumor size in rats inoculated with encapsulated Dox at any concentration, it was shown that insonated tumors were smaller than non-insonated tumors ($p = 0.0062$) [196]. Also, rats that received 2.67mg/kg Dox encapsulated in a NanoDeliv^{TM} carrier and were exposed to 20-kHz and 70-kHz US for 1 h, showed a significant decrease ($p = 0.0061$) in the size of subcutaneous tumors in the hind leg when compared to control tumors in the contralateral leg [196]. Furthermore, the drug was retained in tumors longer and in higher concentrations than in any other tissue, which suggests drug accumulation by the EPR effect with a maximum concentration observed at 12 h [199].

In follow-up experiments using a higher frequency, Staples and co-workers showed a slower growth ($p = 0.0047$) of insonated tumors exposed to NanoDeliv^{TM}-encapsulated Dox, for 15min exposures of both 20-kHz and 500-kHz US [200]. In a more recent study using the same model and 500-kHz US, a tumor regression was observed in the sonicated tissue ($p = 0.001$), even though there was only a slightly greater amount of Dox in the tumor tissue [197]. Because the slight increase in Dox concentration correlated with a large decrease in tumor growth, Staples et al. postulated that more is happening than simple Dox release, and that perhaps cell membranes were being stressed in vivo similar to the in vitro situation. This study also investigated the distribution of Dox in several organs at various times after the Dox-NanoDeliv^{TM} injection and insonation [197]. It was observed that 30 min after the injection the concentration of Dox in the insonated tumor was higher ($p = 0.055$) and that the tumor grew more slowly ($p = 0.0047$). At 12 h and beyond, the insonated and control tumors had Dox concentrations that were not significantly different ($p = 0.988$). Organs and tissues such as the heart, kidneys, liver and muscle had negligible Dox concentrations within 1 week of treatment compared to the high levels that persisted in the tumors. A subsequent study showed that multiple weekly administrations of this drug-delivery system caused significant drug accumulation in the heart, but not in the liver, skeletal leg muscle, or tumors, over the course of 4 weeks

[199]. Application of US alone or the use of the empty NanoDeliv™ micelles did not have any effect on the tumor growth or the lifespan of the rats.

Similar studies have been done in mouse models by other groups. By using fluorescently labeled unstabilized and PEGdiacylphospholipid-stabilized Pluronic® P105 in mice, Gao and co-workers studied the effect of insonation on micellar accumulation inside cells [2]. Ultrasound at 1 or 3 MHz was applied for short periods of time (30 s) to ovarian cancer-bearing nu/nu mice, and this enhanced the accumulation of micelles at the tumor site. A subsequent study by the same group [159] using Dox encapsulated in pure and mixed Pluronic P-105, PEG2000-diacylphospholipid, and poly(ethylene glycol)-co-poly(beta-benzyl-l-aspartate) (PEGb-PBLA) micelles, showed an 8-fold increase in the intracellular Dox uptake upon the application of 30 s of US (1 MHz) in ovarian cancer cells (A2780) in a mouse model. Rapoport and co-workers used flow cytometry to study tumor tissues excised from mice inoculated with Dox encapsulated in Pluronic® P105 micelles [82]. This work showed that micelle accumulation was significantly higher in ultrasonicated tumors than in non-insonated ones. Additionally, they reported that encapsulated Dox did not accumulate in the heart, which would ameliorate concern about the welldocumented cardiotoxicity of this drug [201]. Rapoport's in vivo research efforts used 1-MHz US since this can be focused more precisely on the tumor site and causes less sonolysis than lowerfrequency US, even though 20–100 kHz frequencies are able to release more Dox from Pluronic® P105 micelles than 1–3 MHz frequencies [12,13,84]. Another independent group in Europe [194] used 5-fluorouracil (5-FU) encapsulated in NanoDeliv™ in combination with US(20-kHz, 3.16W/cm^2, 30s) and showed a significantly reduction ($p = 0.0034$) in the tumor (human colon cancer) volume in Balb/c nude mice, when compared to the non-insonated tumor. Additionally the authors reported an even more significant reduction in tumor volume at higher drug concentration.

Howard and co-workers used a micellar Paclitaxel delivery system with US to treat a drug resistant breast cancer tumor cell line [150]; they observed a 20-fold increase in drug uptake when comparing sonicated and non-sonicated samples. Furthermore, the injection of this Paclitaxel formulation for three consecutive weeks in conjunction with US activation (30 s of 1-MHz insonation at 34W/cm^2) resulted in the complete regression of the MCF-7/ADM tumors in nu/nu mice.

A mouse model of breast cancer was used to study the effect of the simultaneous application of 28-kHz and 3-MHz frequency US after the intravenous administration of Dox, free or in stabilized P105 micelles [202]. The Dox concentrations in various tissues were measured 24 h after the treatment. Mice who received a combined US + micellar Dox had nine times more Dox in the tumors than mice receiving free Dox, and three times more than mice receiving micellar Dox but no US. The Dox concentration in non-tumor tissues was lower when micellar Dox was injected than with free Dox. These results support the hypothesis that micellar Dox is extravasated in the tumor and that insonation further increases Dox retention and/or uptake in the tumor tissue. Other studies suggested that US alone can cause extravasation [203–205].

In the study by Chen and co-workers [191] concerning the DTXloaded P105/F127 mixed micelles, they reported successful results in vivo in rat and mice models. The pharmacokinetic study showed that the micellar drug system had a longer circulation time, and that the tumor inhibition rates were higher compared to the free drug. Their study showed promising results and the potentiality of using this system to overcome MDR in lung cancer.

The toxicity and antitumor activity of drug–block copolymer conjugates has also been studied in vivo. The PEG-P[Asp(ADR)] block copolymer developed by Yokoyama and co-workers [101] was tested against five solid tumors in mice, and it was observed that it correlated with a higher antitumor activity than the free ADR (Dox). The conjugated drug-copolymer was also found in blood at much higher concentrations and with a longer half-life than the free drug. Compared to the free drug, it was observed that lower levels of the conjugate accumulated in the heart, lungs and liver, while much higher levels were found in the tumor [206].

In conclusion, many polymeric micellar systems are under investigation in preclinical studies as possible anti-cancer therapeutics. Interestingly, five micellar formulations have already been or are being tested in clinical trials, using drugs such as Paclitaxel or Dox [75].

4.2.4. Mechanisms of acoustically triggered release of micellar drug carriers

The drug release from micelles described previously is most probably caused by the cavitational oscillations and subsequent collapse of gas bubbles in the ultrasonic field. The physics of the interaction between the oscillating gas bubbles and the nanoparticles has been studied extensively and the thresholds of acoustic intensity that produce enough shear on the particles to release the chemotherapeutic drug has been reported [46,145,147].

But how does the US enhance the uptake of drugs by the cells, both in vitro and in vivo?

Three possible mechanisms have been postulated to account for acoustically activated drug delivery from polymeric micelles. These include:

(i) the release of the drug from the micelles using ultrasonic cavitational events which is followed by passive transport process into the cancer cells;
(ii) the upregulation of endocytosis stimulated by cavitationrelated phenomena and subsequent increased uptake of the
drug-containing micelles into the cells;
(iii) the perturbation of the cell membrane leading to the passive transport of the chemotherapeutic drug, either in free/released or micelle-encapsulated form, into the cells.

The first hypothesis postulates the acoustic release of the therapeutic agent from the micelles outside of the cells, creating a concentration gradient across the cell membrane and promoting its transport into the cells by simple diffusion and/or cellular uptake mechanisms such as endocytosis. To test this mechanism, the Pitt group carried on several studies [13,14,178]. Some of the end hydroxyl groups of Pluronic® P105 were labeled with a fluorescein derivative that fluoresces at a different wavelength than the drug (the derivative fluoresced at 550 nm, while Dox fluoresced at 588 nm). A human promyelocytic cell line (HL-60) was incubated with Dox encapsulated in the fluorescein-labeled P105 micelles, without and with insonation. It was observed that both Dox and the labeled micelles appeared inside the treated cells. The labeled P105 was measurable inside the cells even in the absence of US.

The measurements were not quantitative enough to determine if US changed the intracellular ratio of Dox to P105. However, these studies refuted the hypothesis that US only causes the external drug release from the micelle, followed by diffusion of the drug only into the cells. The P105 was found inside the cell. The question still lingered of whether the labeled micelles (non-loaded or drug-loaded) entered into the cell cytosol through holes in the membrane or via endocytosis.

The second hypothesis was that US up regulates endocytosis and pinocytosis so that entire micelles with the drug enter the cell. A receptor-mediated endocytosis route was disqualified as a possible mechanism because it is unlikely that HL-60 cells possess receptors for Pluronic® micelles. The hypothesis that nonspecific endocytosis or pinocytosis, by which small volumes of extracellular fluid enter the cell via membrane invaginations and fuses with acidic lysosomes, was tested using Lysosensor Green, which fluoresces more strongly at acidic pH, as described previously [178]. The results obtained in this experiments rejected the hypothesis that US upregulates pinocytosis or non-specific endocytosis in general; but these observations are in contradiction with the results obtained by Rapoport's group [82,119,158], Sheikov et al. [180], and other groups [181,182] using different cell lines, as described in Section 4.2.2. Direct experimental evidence of the uptake of micelles by US-enhanced endocytosis has not yet been observed, hence this issue remains unresolved. It is possible that different cell lines respond differently to the US stimulus, and thus a global conclusion cannot be generalized based on the results of these experiments.

The third hypothesis, that micelles enter the insonated cells via holes in the membrane, is supported by several studies, including the ones by the Pitt group, described previously [13,14,178]. The study with the model calcein, also described previously [187], reported that collapse cavitation induced by US was implicated in the disruption of the cell membrane. Several other reports support the US-induced sonoporation, including studies that show electron micrographs of damaged cell membranes [7,8,183,184]. In some cases the disruptions are repairable and may not cause the death of the treated cells. Saito et al. [207] showed an increase in the permeability of corneal endothelium cells upon exposure to US. This increase was reversible, and the cells regained their membrane integrity several minutes after the acoustic treatment.

The group of Tachibana has also presented direct evidence of the increase in cell membrane permeability and skin porosity caused by insonation [5–8,10,208–210]. Similarly, Schlicher et al. have shown that the accumulation of calcein in prostate cancer cells was caused by membrane disruptions or pores induced by US. In their analysis, they used flow cytometry coupled with electron and fluorescence microscopies to show the micropores [22]. Prentice and co-workers showed that single cavitation events induced by 1-MHz US can cause holes in the cell membrane, as directly evidenced by atomic force microscopy [183]. Therefore, this third mechanism is supported. This mechanism postulates that the US-induced permeabilization of the cellular membrane is followed by transmembrane transport of micelle-encapsulated drugs. As for the first two mechanisms, there is evidence that US disrupts the core of polymeric micelles (most probably by strong shear stresses) and causes the drug release, while enhanced endocytotic events are a possibility [19]. The main role of cell membrane perturbation (Fig. 4) is consistent with the in vivo observation that insonation of tumors with Dox-loaded NanoDeliv™ micelles produce a minimal increase in the drug concentration in the tumor site, but a significant decrease in the tumor growth rate [197]. Furthermore, the observation that NanoDeliv™ micelles only release about 3% of Dox when insonated in vitro further supports the hypothesis that the US-induced release of the drug from the micelles may not be the main factor in reducing the tumor growth in vivo [147].

5. Liposomes and eLiposomes

5.1. Liposomes as drug delivery systems

The use of liposomes in drug delivery systems is actually fairly recent, dating from the mid-1960s when pharmaceutical chemists developed methods by which surfactants could form bilayer membranes, and realized that these membranes could self-assemble into vesicles that entrap hydrophilic contents on the inside that could not escape quickly through the bilayer membrane. Thus hydrophilic drugs could be encapsulated within a liposome and

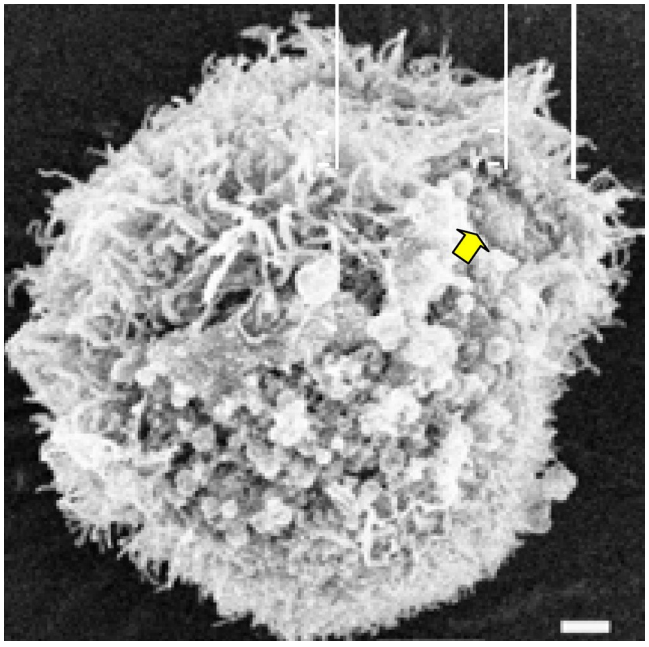

Fig. 4. A SEM micrograph showing a micropore in the cell member of a cancer cell after sonication at 0.54 MHz. Taken with permission from [184].

be transported in an aqueous system (like blood) without being released instantly upon dilution into that aqueous system. The therapeutics could diffuse slowly through the membrane for controlled release over time, or the membrane could be ruptured and the drug released suddenly by some event that ruptured or permeabilized the membrane. There are several comprehensive books and reviews on liposomal drug delivery that can be consulted [211–213].

Drug encapsulation within liposomes presents a type of conundrum. More robust and stable liposomes could contain contents without leakage, but when the time and place of delivery arrived, release of the drug was more difficult. To accomplish both stable sequestration and on-demand release, the liposome chemistries were tweaked to make the membrane permeability and/or stability sensitive to temperature [214,215], pH [216,217], and other environmental changes or triggers [218,219].

These triggers can be further divided into those that are generated passively and actively (using a ligand). Passive triggering occurs due to changes in the tissue environment so that drug release from the liposome occurs naturally without any external control. These include changes in pH, temperature, or the concentration of enzymes, all of which may occur in tumors or at the sites of inflammation. These triggers are ideal to treat disseminated diseased tissues, such as metastatically disseminated secondary tumors. Triggering is useful when the site of release has been identified, and then the trigger can be applied in a controlled manner, usually from outside the body. These include triggering to release the contents of the liposome by light [219], US, magnetic fields [191,220,221], or other physical stimuli [222] that can be focused on a targeted volume and controlled in time. The balance of this section will review the application of US as a trigger to release the contents of liposomes.

5.2. Ultrasonic drug release from liposomes and eLiposomes

5.2.1. General description of acoustically triggered release from liposomes

As described above and in Section 3.2, liposomes consist of a lipid bilayer membrane surrounding an aqueous interior. In theory, liposomes are even more transparent to US than micelles because there is no hydrophobic core having different acoustic properties. Furthermore the absence of a hydrophobic phase eliminates the potential for the liposome to store large amounts of dissolved gas that could initiate bubble formation. To interact with US, liposomes must contain an internal gas bubble [223–225] or a liquid phase [57–60,226–228] that can turn to a gas bubble upon insonation; or bubbles can be attached to the exterior of the liposome [229], nested inside [230], or reside in the general proximity of liposomes [231,232]. In all of these cases, ultrasonically induced cavitation of the gas phase produces volume changes and large shear stresses that can perturb the bilayer structure, creating small pores for enhanced permeability or producing large-scale disruption of the entire liposome, leading to instant release of the contents. Fig. 5 illustrates some of the acoustically sensitive liposomes that have been reported in the literature. They will be discussed below.

In non-cavitational applications, US has also been used to thermally heat a volume of liquid containing liposomes with specially designed membranes that have a thermal transition temperature just above body temperature [214,233,234]. Heating above this transition temperature greatly increases the membrane permeability with respect to the therapeutic release.

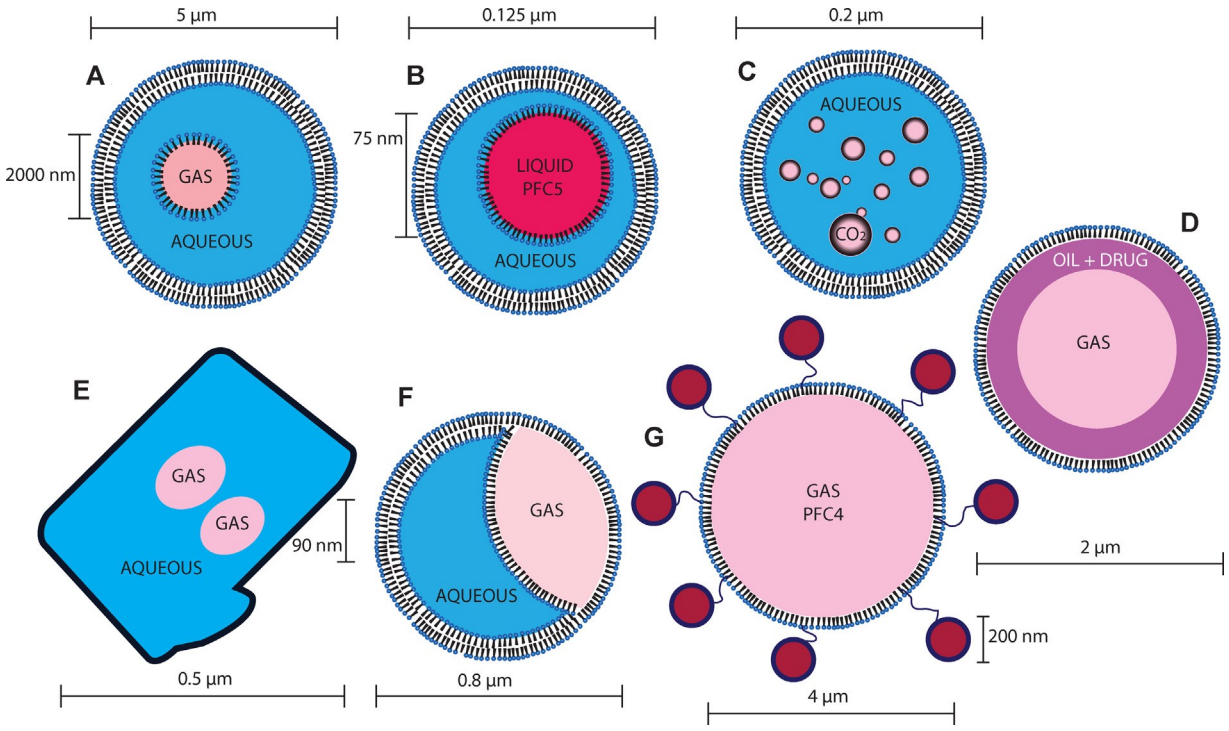

Fig. 5. Various ultrasound-sensitive liposome constructs reported in the literature. (A) Liposome-nested-nanobubble (adapted from [230]). (B) eLiposome (adapted from [59]). (C) CO_2-gas-generating liposome (adapted from [237]). (D) Acoustically active liposphere (adapted from [223]). (E) Bubble liposome (adapted from [255]). (F) Echogenic liposome (adapted from [240]). (G) Liposome-loaded microbubble (adapted from [269]). Relative sizes are not to scale, but are indicated by the size bars for each construct.

These constructs are called "thermally sensitive liposomes" (TSL) and have moved toward clinical evaluation. Both aspects of ultrasonically activated therapeutic delivery are reviewed below.

5.2.2. Formulation of and triggered release from liposomes by ultrasound in vitro

5.2.2.1. Gas bubbles in liposomes. There are various methods to stabilize a gas bubble nested inside a liposome. One of the challenges is that the gas bubble will be very small, usually less than 2 m in diameter. Bubbles this small have an extreme amount of Laplace pressure compressing the interior gas, and unless there is a stable surfactant layer coating the bubble to provide mechanical rigidity and reduce the interfacial tension, the high pressure will cause the gas to dissolve into the surrounding liquid, and the bubble will vanish. Bubble stabilization is required as most applications require smaller bubbles.

Ibsen et al. prepared a fairly simple vehicle composed of a liposome of about 7 m in diameter containing a micron-sized bubble along with the drug [230,235]. The construct, called a nested bubble, was made by sonicating a mixture of perfluorohexane (PFC6) and air into an aqueous phospholipid/glycerol/propanediol solution, forming fairly stable suspension of bubbles. This was next mixed into a phospholipid/cholesterol solution in ethanol. Then water was added to form and close liposomes around the stable bubbles. Soluble drugs, proteins or particles could be added to the bubble solution and encapsulated by the liposomes. Exposure of these constructs to 2.25 MHz US of 1–1.5 MPa caused violent cavitation of the gas bubble which led to the rupture of the liposome.

Another group made stable liposomes and then sonicated them in the presence of perfluoropropane (PFC3) gas, forming what they called "gas-cored liposomes" [236]. Electron microscopy showed that these are somewhat spherical constructs on the order of hundreds of nm in diameter, but it is uncertain if these are truly liposomes containing a gas bubble inside, or if they are stable nanobubbles (with negligible aqueous interior).

Another technique to place a bubble inside a liposome is to generate gas by a chemical reaction within the liposomes. This has been done by more than one research group using a bicarbonate

solution inside the liposome, and then decreasing the pH to form carbon dioxide gas [237,238]. This is particularly useful in forming gas bubbles after the liposome has entered a region of low pH, such as an endosome or lysosome or the region of some tumors. The liposomes become echogenic, thus revealing possible locations of tumors. Application of US to

the echogenic liposomes causes rupture and release of the liposome content.

A similar CO_2 generation technique has been demonstrated elevating the temperature, without changing the pH [239]. Usually the tumor environment is a few degrees warmer than normal body temperature and this can form CO_2 gas in a liposome loaded with Dox. Often tumors are both warm and slightly acidic, both of which will promote CO_2 generation to provide echogenicity and payload delivery.

In the gas-containing liposomes described above, gas bubbles were specifically added to or formed within the liposome. Several authors have made liposomes that are echogenic and acoustically active from phospholipids, cholesterol and sometimes carbohydrates by more subtle or passive techniques of introducing bubbles [240–246]. Their acoustic behavior suggests that a gas phase is present in or adjacent to the liposome. In one procedure, these liposomes are formed by standard film hydration techniques and then lyophilized for storage. The liposomes were rehydrated using "airsaturated deionized water" [247]. It is thought that gas dissolved in the rehydrating solution is the source of the gas bubbles that appear to be stabilized by the lipids [241,248]. Similarly, lyophilized liposomes were saturated with PFC3 gas and then rehydrated with distilled water to form acoustically active liposomes [249].

In a second type of procedure, the liposomes were formed by sonication and then placed under a pressurized atmosphere of the desired gas (air or perfluorocarbon). Then the sample was frozen for a time and thawed [70,240]. The thawed sample was echogenic and acoustically active. It is postulated that during the freezing process the dissolved gas comes out of solution and is surrounded and stabilized by the phospholipids. This construct is stable, survives the thawing process, and provides gas bubbles adjacent to or within the liposomes. This process has developed very useful echogenic liposomes which have been used to deliver tissue plasminogen activator to dissolve clots [250] and to deliver genes [249] and other therapeutics [244]. The activation thresholds for in vitro release have been measured [251].

A similar construct called a "bubble liposome" was developed by Suzuki et al. [224,225,252–255]. This echogenic liposome is made from PEG-containing phospholipids using a reverse phase evaporation process. They were extruded to 200 nm and the liposome suspension was placed in contact with pressurized PFC3 gas and sonicated in a bath sonicator for 5 min to form the bubble liposomes. Their hypothesis is that during bath sonication, the pressurized gas diffused into the solution and collected within the liposomes, forming stable gas bubbles of about 100 nm in diameter that could be acoustically activated to burst the liposome. A similar construct has been made using perfluoropentane (PFC5) gas [228]. These bubble liposomes have been used in a wide variety of applications for gene delivery [224,225,252–259].

One advantage of bubble liposomes over echogenic liposomes is that the bubble liposomes are generally on the order of hundreds of nanometers in size, compared to micron sizes for echogenic liposomes. The smaller size allows for extravasation into tumors and for endocytosis.

5.2.2.2. Liquid droplet in liposome. The desire for very small sized vesicles brings us to another type of construct in which a gas bubble is not pre-existing, but which forms upon a triggering event such as insonation. The absence of a gas bubble allows constructs of less than 500 nm to be formed, which can be beneficial when the construct is designed to be extravasated or endocytosed. Lattin et al. developed a construct called an emulsion-liposome, or "eLiposome", consisting of a liposome with emulsion droplet(s) inside [57,58]. They created small stable emulsion droplets of PFC6 or PFC5 by sonication with a probe sonicator on ice. The emulsion

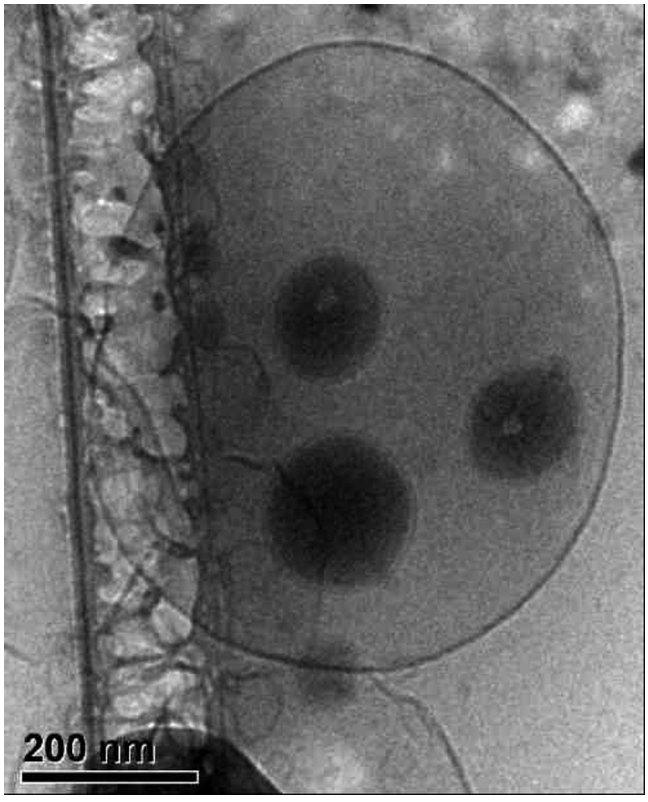

Fig. 6. A cryo-TEM image of an eLiposome encapsulating three emulsion droplets.
Taken with permission from [57].

was then mixed with a suspension of phosphatidylcholine lipid sheets, created by adding ethanol to small liposomes [260]. After physically mixing the lipid sheets and emulsion, the combination

was heated above the order-disorder transition temperature of the lipid sheets, and they spontaneously folded into large liposomes, trapping some of the perfluorocarbon (PFC) emulsion droplets inside. Surprisingly the heating process did not change the PFC droplets to gas, which was attributed to the high Laplace pressure of the small emulsion droplets. The eLiposomes were extruded to a small uniform size, and apparently at least some of the emulsion droplets remained inside since the application of US caused the eLiposomes to burst and release calcein [57]. They were also visualized by cryogenic transmission microscopy (Fig. 6).

The theory behind this mode of delivery is that the liquid PFC droplets within the liposome remain stable below the normal boiling point and even a few degrees above their boiling point (due to Laplace pressure). During insonation, the local pressure drops below the vapor pressure of the liquid nanodroplets, causing them to expand to gas. This phenomenon is called "acoustic droplet vaporization" and has been reviewed elsewhere [261–263]. The increase in volume within the eLiposome is sufficient to disrupt the phospholipid bilayer membrane, and the enclosed contents are released. Furthermore if the ultrasonic pulse is long, the gas bubble so formed may continue to cavitate, thus creating shear forces and convection that may destroy the vesicle and further disperse the contents. The acoustic phase transition of perfluoroemulsions was studied in detail [264] and modeled later [265].

The same lab developed two other techniques to envelope emulsion droplets within liposomes, one of which was done by hydrating a dried lipid layer with a suspension of PFC emulsion droplets, and the other by mixing the PFC emulsion with preformed phosphatidylcholine liposomes, and applying mild sonication on ice. Apparently the mild sonication opens up the liposomes, and the emulsion droplets diffuse inside and are trapped [59]. These latter constructs were loaded with calcein and DNA and then labeled with folate molecules to promote endocytosis into cancer cells. Once endocytosed, US was applied and the conversion of liquid PFC to gas caused sufficient expansion to burst both the eLiposome and endosome and deliver the calcein and plasmids to the cell cytosol [60,266]. Doxorubicin and paclitaxel have also been delivered to cells with this technique [60,266–268].

5.2.2.3. Liposomes attached to bubbles. The next general class of constructs consists of small liposomes that are attached to larger gas bubbles. During insonation the bubble cavitates violently, and the resulting shear forces and shock waves disrupt the nearby liposome membrane and release the enclosed therapeutic. The liposomes are usually loaded with the therapeutic and are as small as 100 nm. The bubbles often contain a PFC gas and are 1–3 m in diameter, so they are too large for extravasation. Attachments between bubbles and liposomes are made by a variety of chemistries, including maleimide-thiol [269–271], biotin-streptavidin [272], and biotin-avidin [229,273]. These constructs have been used to deliver a wide variety of therapeutics, as will be discussed later.

5.2.2.4. Other constructs. There is a construct called an "acoustically active liposphere" that might sometimes be confused with a liposome. It is made from soy oil, phospholipids and drugs, and then mixed vigorously with perfluorobutane gas (PFC4). It is considered a gas bubble inside a layer of oil and stabilized by a layer of phospholipid [223,274]. It differs from other echogenic liposomes in that it is not designed to have an aqueous interior phase. It has an oily internal phase that is useful in carrying hydrophobic drugs.

5.2.3. In vitro delivery of therapeutics to cell cultures

As the first step on the pathway to clinical application, delivery of therapeutics to cancer cells lines in vitro has been explored with all of the constructs described above. The reports are too numerous to be all compiled in this review, but selected applications will be highlighted.

5.2.3.1. Thermally sensitive liposomes with HIFU. Thermally sensitive liposomes have been investigated for at least a decade, and they are in preparation for clinical trials for delivery of Dox using high intensity focused ultrasound (HIFU). Most of the in vitro preliminary work has been related to the examination of the HIFU parameters for release of Dox [275–277]. There is an interesting report of combining thermally sensitive liposomes with bubbles to release a dye to cells in vitro [232]. The greatest cell uptake of the dye was in a two-step approach of first heating the temperature sensitive liposomes with HIFU, and then adding Sonovue microbubbles and applying US again. The authors proposed that hyperthermia released the dye, and then the gas bubbles produced sonoporation of the cells for enhanced cellular uptake.

5.2.3.2. Bubble liposomes. As mentioned above, bubble liposomes have been employed for plasmid delivery, and also for small molecule delivery to cells. For example, hepatocyte growth factor gene was delivered to cultured cardiocytes [278], and the luciferase (Luc) gene was successfully delivered to human embryonic kidney carcinoma cells [279,280] using 2.5-and 2.0-MHz US, respectively. siRNAs targeting the protein luciferease and green fluorescence protein were successfully delivered to several cancer cell lines using bubble liposomes and 2-MHz insonation [253]. Likewise siRNA targeting luciferase was delivered to bladder

cancer cells [281]. Bubble liposomes were used to deliver Dox to a murine osteosarcoma cell line [9].

5.2.3.3. eLiposome for cytosolic delivery. eLiposomes are designed to deliver their payload to the cytosol since they are endocytosed and then activated by US to break both the liposome and endosome. Folated eLiposomes successfully delivered calcein and a green fluorescent protein (GFP) plasmid to HeLa cells [226,266]. When the folate ligand (which binds the eLiposome to a folate receptor and induces endocytosis) was absent, negligible drug delivery or plasmid expression was observed. It is noteworthy that GFP expression was observed in every cell, indicating high transfection efficiency, even though plasmids have little to no diffusivity in the cytosol, and no nuclear location sequences were applied to the plasmids. It could be that the PFC bubble that was generated by insonation continued to cavitate after it ruptured the liposome and endosome, and the subsequent cavitation promoted transport of the plasmids to the nucleus. This eLiposome construct is ideal for delivering molecules that have their action in the cytosol, such as the delivery of siRNA or paclitaxel.

5.2.3.4. Liposomes attached to bubbles. There are only a couple of reports of successful delivery from liposomes attached to insonated microbubbles. In one report a hydrophobic fluorescent molecule (model drug) was delivered to human prostate cancer cells using 1.6-m-diameter PCF4 bubble and 2.25-MHz insonation [229]. In another report, liposomal Dox was delivered to human glioblastoma cells using 3.6-m-diameter PFC4 bubbles and 1 MHz-US [269].

5.2.4. Ultrasonically activated delivery from liposomes in vivo

A much more challenging application is the ultrasonic activation of the liposomes in animal experiments, requiring equipment for focusing the US on a target site, and the safe formulation of the liposome.

Perhaps the most work has been done with temperaturesensitive liposomes, many of which contain Dox. High intensity focused ultrasound was used in several studies to thermally release the drug to tumors [233,275,282–287], muscle [286,288,289] and even bone marrow [286,287]. Studies in mice, rats and rabbits have been recently reviewed [214]. One of the challenges with HIFU in vivo is overheating the tissues. Hijnen [290] reviews applications in which magnetic resonance imaging (MRI) is used during the HIFU procedure to monitor and control the local temperature of the target tissue [290]. In general the results of in vivo experiments show that localized drug delivery from temperature-sensitive liposomes can be achieved, and that tumor regression is often observed. In one notable report, HIFU activation of delivery of a Cu-Dox from a temperature sensitive liposome resulted in complete regression (8 months tumor-free) of metastatic breast cancer tumors in a mouse model [291].

Echogenic liposomes have been employed in a variety of animal models. The have been used to deliver tissue plasminogen activator to thrombi in a rabbit model [247,250], and nitric oxide in rabbit and rat artery models [292–294], and a swine model of atherosclerosis [295]. They have also delivered xenon gas in a stroke model in a rat [296]. This application of delivering therapeutic gases from echogenic liposomes is rather unique and appears to be effective. The gases are loaded into the liposomes during the process of making them echogenic.

Publications of bubble liposomes over the past 6 years have focused mostly on gene delivery, but there have been some publications on drug and protein delivery. Marker genes of GFP and Luc have been delivered to the rat eye subconjunctiva (GFP) [224], and to muscles and human bladder tumors in mice (Luc) [281,297]. Delivery of a therapeutic gene, interleukin-12, was reported in a mouse tumor model [252,254]. In these reports the plasmids apparently associated with the negatively charged surface of the bubble liposome. In all cases reported, the transfection was successful, and was attributed to bubble cavitation enhancing the transport of the genetic material into the cell. In other studies, Dox was successfully delivered to a mouse osteosarcoma [9], and recombinant tissuetype plasminogen activator was delivered to thrombosed rabbit iliofemoral arteries [298]. Recanalization was achieved in 90% of the arteries.

The last construct that we will discuss in this section is the conjunction of therapeutic-containing liposomes to stable microbubbles. While there are many report of in vitro research, there are only a few reports of in vivo delivery. Yang et al. used a liposome-bubble assembly to deliver microRNA to the livers of rats with hepatic fibrosis [273]. The delivery produced a sequence of proteomic and therapeutic changes. Another report showed that paclitaxel was successfully delivered to breast cancer tumors in mice. Lastly a group from the Netherlands delivered a marker dye to the legs of mice [270].

5.2.5. Clinical trials

As of this writing, there are no published reports of clinical trials in peer-reviewed publications of liposomes combined with US. However, there is information on the web pages of interested agencies like the NIH ClinicalTrials.gov and other web pages. To date, only four clinical trials have been started on the product ThermoDox, made by Celsion Corporation of Lawrenceville, New Jersey. ThermoDox is a thermally sensitive liposome

containing Dox. There is a Phase 3 trial of Thermodox to treat hepatocellular carcinoma, with triggering by radio frequency (RF) ablation (no US). The control is RF ablation without any drug delivered. The trial started in 2008 and is expected to end in 2015. In January of 2013, Celsion announced that this trial had not met the primary goal of demonstrating persuasive evidence of clinical effectiveness, but the trial would continue to evaluate the secondary goal of increased overall survival. There was a Phase 1 study on a similar topic, the combination of Thermodox with RF ablation to treat primary and metastatic tumors of the liver; it was initiated in 2007 and completed in 2009, but no study results were posted. We presume that it was sufficiently successful that the Phase 3 study mentioned above was approved.

A Phase 1 study was completed in 2011 investigating the use of Thermodox and RF ablation to treat locally recurrent breast cancer. Likewise, a Phase 2 study was completed in 2013 also on the use of Thermodox and RF ablation to treat metastatic colorectal cancer. No results were posted or published yet on either of these studies.

Two studies are recruiting (as of 2014) but not yet started. One is a Phase 1&2 study of combining Thermodox with RF ablation to treat reoccurring breast cancer at the chest wall. The other is a Phase 3 study of MRI-guided HIFU and Thermodox to treat bone metastases.

We find it encouraging that a liposomal delivery system has made it to the planning stages of a clinical trial using HIFU. The combination of HIFU with MRI-guidance of tumor location and ultrasonic heating is expected to show promise. Future steps would include delivery of other drugs using US, and using liposomes that contain gas for activation.

6. Solid nanoparticles and ultrasound

Solid nanoparticles per se have very little interaction with US other than reflecting sound from their surface. As mentioned previously, in a mixed suspension of bubbles and particles more dense than the surrounding fluid, secondary radiation forces will move the particles toward the bubbles where they may be sheared. It is possible that bubble cavitation near the particle may erode the surface.

Nanoparticles (NPs) are often used to carry drugs (particularly drugs that are not soluble in water) and genetic material (DNA plasmids, RNA, siRNA, etc.) that must be protected from degradative enzymes. The most common application of US in solid nanoparticle delivery is to attach the nanoparticles to the surface of microbubbles and then cavitate the bubbles. An excellent review has recently been published on this topic [299]. Herein we will only highlight some of the key features of the use of US in nanoparticle delivery.

6.1. Magnetic particles and ultrasound

There are several reports of delivering therapeutics associated with magnetic and paramagnetic particles on microbubbles as well as independent of bubbles. These particles can be “guided” or localized by external magnetic fields, and they can also be imaged by MRI techniques. There are two general approaches to this delivery technology: attached to microbubbles or unattached. An example of magnetic particles attached to microbubbles is found in a report of the delivery of plasmids and iron oxide NPs on the surface of 4.3-m-diameter PFC microbubbles [300]. The constructs were injected into mice and collected in a dorsal skin-fold chamber with an electromagnet, and then insonated at 1 MHz for 30 s. Successful transfection was obtained.

In a novel application, metal stents were coated with Ni to make them magnetic, and placed in cell cultures of porcine endothelial and smooth muscle cells [301]. Iron oxide NPs were coated with rapamycin and attached to PCF3 bubbles. A field from a permanent magnet caused the magnetic bubbles to attach to the Ni-coated stent. Then US was applied from a probe-type sonicator and the bubbles burst to release the drug locally to the adjacent cells.

In other applications, US and microbubbles were used to first open the blood–brain barrier in rats [302,303] or pigs [304], and magnetic NPs were directed to the lesion sites with external magnets. A drug coated on the NPs was successfully delivered to a rat glioma, which suppressed tumor growth [305].

6.2. Other nanoparticles and ultrasound

Poly(lactic-co-glycolic acid) nanoparticles were loaded with the anticancer agent 5FU, attached to albumin-shelled microbubbles, and delivered to mice hosting a glioma model [306,307]. Insonation at 1 MHz caused uptake of the particles, a reduction in tumor growth and an increase in survival.

In an example of NPs not attached to microbubbles, small 20-nm NPs (quantum dots) were delivered into breast cancer spheroids grown in vitro by applying pulsed US [308]. Optison microbubbles were added, and there was a 6- to 20-fold greater penetration into the spheroids compared to controls. Although the particles were not attached to the microbubbles, the cavitation events appeared to propel the particles into the spheroids.

7. Conclusion

Cancer is one of the deadliest diseases that plague our modern era. It has claimed the lives of several millions worldwide. Several therapies are effective in combating malignant growth of which one of the most extensively used is chemotherapy. However, this method is plagued with well-known undesirable side effects. These side effects are caused solely because of the nonspecific nature of this treatment since the drug is able to

interact with healthy as well as abnormal tissue. A reasonable solution to overcome these limiting side effects is to use "smart" molecular vehicles to sequester the therapeutic drug in a package and release it to the specific tumor site at the appropriate time. In so doing, the drug will have minimal interactions with healthy cells in the body, thus reducing many of the unwanted side effects associated with conventional chemotherapy, increasing the efficacy of the drug, and greatly improving the quality of life for cancer patients.

This paper reviewed three classes of nanosized drug delivery carriers currently investigated as acoustically activated vehicles for chemotherapy, namely solid nanoparticles, liposomes and micelles. The only clinical trials have been conducted to test the feasibility of administering thermally sensitive liposomes and high intensity US to treat cancer. However, there are several in vivo studies that suggest that improved results, with potentially fewer side effects, are in the pipeline using these promising and novel drug delivery systems.

Acknowledgement

The authors acknowledge the financial support of the Faculty Research Grant Type 1 (FRG1-2012), from the American University of Sharjah.

References

[1] P.A. Dijkmans, L.J. Juffermans, R.J. Musters, A. van Wamel, F.J. ten Cate, W. van Gilst, C.A. Visser, N. de Jong, O. Kamp, Microbubbles and ultrasound: from diagnosis to therapy, Eur. J. Echocardiogr. 5 (2004) 245–256.

[2] S. Mitragotri, Healing sound: the use of ultrasound in drug delivery and other therapeutic applications, Nat. Rev. Drug Discov. 4 (2005) 255–260.

[3] D. Peer, J.M. Karp, S. Hong, O.C. Farokhzad, R. Margalit, R. Langer, Nanocarriers as an emerging platform for cancer therapy, Nat. Nanotechnol. 2 (2007) 751–760.

[4] K.E. Uhrich, S.M. Cannizzaro, R.S. Langer, K.M. Shakesheff, Polymeric systems for controlled drug release, Chem. Rev. 99 (1999) 3181–3198.

[5] S. Miura, K. Tachibana, T. Okamoto, K. Saku, In vitro transfer of antisense oligodeoxynucleotides into coronary endothelial cells by ultrasound, Biochem. Biophys. Res. Commun. 298 (2002) 587–590.

[6] M. Sivakumar, K. Tachibana, A.B. Pandit, K. Yasui, T. Tuziuti, A. Towata, Y. Iida, Transdermal drug delivery using ultrasound-theory, understanding and critical analysis, Cell. Mol. Biol. (Noisy-le-grand) 51 (Suppl.) (2005) OL767–OL784.

[7] K. Tachibana, T. Uchida, K. Ogawa, N. Yamashita, K. Tamura, Induction of cellmembrane porosity by ultrasound, Lancet 353 (1999) 1409.

[8] K. Tachibana, T. Uchida, K. Tamura, H. Eguchi, N. Yamashita, K. Ogawa, Enhanced cytotoxic effect of Ara-C by low intensity ultrasound to HL-60 cells, Cancer Lett. 149 (2000) 189–194.

[9] Y. Ueno, S. Sonoda, R. Suzuki, M. Yokouchi, Y. Kawasoe, K. Tachibana, K. Maruyama, T. Sakamoto, S. Komiya, Combination of ultrasound and bubble liposome enhance the effect of doxorubicin and inhibit murine osteosarcoma growth, Cancer Biol. Ther. 12 (2011) 270–277.

[10] N. Yamashita, K. Tachibana, K. Ogawa, N. Tsujita, A. Tomita, Scanning electron microscopic evaluation of the skin surface after ultrasound exposure, Anat. Rec. 247 (1997) 455–461.

[11] G.A. Husseini, R.I. El-Fayoumi, K.L. O'Neill, N.Y. Rapoport, W.G. Pitt, DNA damage induced by micellar-delivered doxorubicin and ultrasound: comet assay study, Cancer Lett. 154 (2000) 211–216.

[12] G.A. Husseini, G.D. Myrup, W.G. Pitt, D.A. Christensen, N.Y. Rapoport, Factors affecting acoustically triggered release of drugs from polymeric micelles, J. Control. Release 69 (2000) 43–52.

[13] A. Marin, H. Sun, G.A. Husseini, W.G. Pitt, D.A. Christensen, N.Y. Rapoport, Drug delivery in Pluronic micelles: effect of high-frequency ultrasound on drug release from micelles and intracellular uptake, J. Control. Release 84 (2002) 39–47.

[14] M.D. Muniruzzaman, A. Marin, Y. Luo, G.D. Prestwich, W.G. Pitt, G.A. Husseini, N. Rapoport, Intracellular uptake of Pluronic copolymer: effects of the aggregation state, Colloids Surf. B: Biointerfaces 25 (2002) 233–241.

[15] G.A. Husseini, W.G. Pitt, D.A. Christensen, D.J. Dickinson, Degradation kinetics of stabilized Pluronic micelles under the action of ultrasound, J. Control. Release 138 (2009) 45–48.

[16] G.A. Husseini, D. Velluto, L. Kherbeck, W.G. Pitt, J.A. Hubbell, D.A. Christensen, Investigating the acoustic release of doxorubicin from targeted micelles, Colloids Surf. B: Biointerfaces 101 (2013) 153–155.

[17] G.A. Husseini, L. Lherbeck, W.G. Pitt, J.A. Hubbell, D.A. Christensen, D. Velluto, Kinetics of ultrasonic drug delivery from targeted micelles, J. Nanosci. Nanotechnol. 15 (2014) 2099–2104.

[18] W.G. Pitt, G.A. Husseini, B.J. Staples, Ultrasonic drug delivery – a general review, Expert Opin. Drug Deliv. 1 (2004) 37–56.

[19] G.A. Husseini, W.G. Pitt, Ultrasonic-activated micellar drug delivery for cancer treatment, J. Pharm. Sci. 98 (2009) 795–811.

[20] W.L. Nyborg, Biological effects of ultrasound: development of safety guidelines. Part II: General review, Ultrasound Med. Biol. 27 (2001) 301–333.

[21] J.A. Rooney, Hemolysis near an ultrasonically pulsating gas bubble, Science 169 (1970) 869–871.

[22] R.K. Schlicher, H. Radhakrishna, T.P. Tolentino, R.P. Apkarian, V. Zarnitsyn, M.R. Prausnitz, Mechanism of intracellular delivery by acoustic cavitation, Ultrasound Med. Biol. 32 (2006) 915–924.

[23] S.A. Goss, R.L. Johnston, F. Dunn, Comprehensive compilation of empirical ultrasonic properties of mammalian tissues, J. Acoust. Soc. Am. 64 (1978) 423–457.

[24] D.O. Draper, J.C. Castel, D. Castel, Rate of temperature increase in human muscle during 1 MHz and 3 MHz continuous ultrasound, J. Orthop. Sports Phys. Ther. 22 (1995) 142–150.

[25] P.E. Huber, J. Debus, Tumor cytotoxicity in vivo and radical formation in vitro depend on the shock wave-induced cavitation dose, Radiat. Res. 156 (2001) 301–309.

[26] P.E. Huber, J.W. Jenne, R. Rastert, I. Simiantonakis, H.P. Sinn, H.J. Strittmatter, D. von Fournier, M.F. Wannenmacher, J. Debus, A new noninvasive approach in breast cancer therapy using magnetic resonance imaging-guided focused ultrasound surgery, Cancer Res. 61 (2001) 8441–8447.

[27] T.G. Leighton, What is ultrasound? Prog. Biophys. Mol. Biol. 93 (2007) 3–83.

[28] X.Q. Lu, E.C. Burdette, B.A. Bornstein, J.L. Hansen, G.K. Svensson, Design of an ultrasonic therapy system for breast cancer treatment, Int. J. Hyperthermia 12 (1996) 375–399.

[29] H.R. Underwood, E.C. Burdette, K.B. Ocheltree, R.L. Magin, A multi-element ultrasonic hyperthermia applicator with independent element control, Int. J. Hyperthermia 3 (1987) 257–267.

[30] A.H. Saad, G.M. Hahn, Ultrasound enhances adriamycin toxicity in vitro, in: J.C. Chato, T.E. Diller, K.R. Diller, R.B. Roemer (Eds.), Heat Transfer in Bioengineering and Medicine, Am. Soc. Mech. Engr. Press, New York, 1987, pp. 28–31.

[31] J. Collis, R. Manasseh, P. Liovic, P. Tho, A. Ooi, K. Petkovic-Duran, Y. Zhu, Cavitation microstreaming and stress fields created by microbubbles, Ultrasonics 50 (2009) 273–279.

[32] P. Marmottant, S. Hilgenfeldt, Controlled vesicle deformation and lysis by single oscillating bubbles, Nature 423 (2003) 153–156.

[33] W.L. Nyborg, Ultrasonic microstreaming and related phenomena, Br. J. Cancer Suppl. 5 (1982) 156–160.

[34] C.E. Brennen, Cavitation and Bubble Dynamics, Oxford University Press, New York, 1995.

[35] D.J. May, J.S. Allen, K.W. Ferrara, Dynamics and fragmentation of thick-shelled microbubbles, IEEE Trans. Ultrason. Ferroelectr. Freq. Control 49 (2002) 1400–1410.

[36] J.A. Rooney, Ultrasound: Its Chemical, Physical, and Biological Effects, VCH Publishers, 1988.

[37] A.R. Williams, D.L. Miller, Photometric detection of ATP release from human erythrocytes exposed to ultrasonically activated gas-filled pores, Ultrasound Med. Biol. 6 (1980) 251–256.

[38] S.B. Stringham, M.A. Viskovska, E.S. Richardson, S. Ohmine, G.A. Husseini, B.K. Murray, W.G. Pitt, Over-pressure suppresses ultrasonic-induced drug uptake, Ultrasound Med. Biol. 35 (2009) 409–415.

[39] E.C. Everbach, I.R. Makin, M. Azadniv, R.S. Meltzer, Correlation of ultrasoundinduced hemolysis with cavitation detector output in vitro, Ultrasound Med. Biol. 23 (1997) 619–624.

[40] K.I. Morton, G.R. ter Haar, I.J. Stratford, C.R. Hill, The role of cavitation in the interaction of ultrasound with V79 Chinese hamster cells in vitro, Br. J. Cancer Suppl. 5 (1982) 147–150.

[41] K.I. Morton, G.R. Ter Haar, I.J. Stratford, C.R. Hill, Subharmonic emission as an indicator of ultrasonically-induced biological damage, Ultrasound Med. Biol. 9 (1983) 629–633.

[42] A.A. Atchley, L.A. Crum, Ultrasound Its Chemical, Physical, and Biological Effects, VCH Publishers, New York, 1988.

[43] M. Delius, Minimal static excess pressure minimises the effect of extracorporeal shock waves on cells and reduces it on gallstones, Ultrasound Med. Biol. 23 (1997) 611–617.

[44] Y.-H. Lee, J.-O. You, C.-A. Peng, Retroviral transduction of adherent cells in resonant acoustic fields, Biotechnol. Prog. 21 (2005) 372–376.

[45] I.V. Larina, B.M. Evers, T.V. Ashitkov, C. Bartels, K.V. Larin, R.O. Esenaliev, Enhancement of drug delivery in tumors by using interaction of nanoparticles with ultrasound radiation, Technol. Cancer Res. Treat. 4 (2005) 217–226.

[46] G.A. Husseini, M.A. Diaz de la Rosa, E.S. Richardson, D.A. Christensen, W.G. Pitt, The role of cavitation in acoustically activated drug delivery, J. Control. Release 107 (2005) 253–261.

[47] V. Sboros, Response of contrast agents to ultrasound, Adv. Drug Deliv. Rev. 60 (2008) 1117–1136.

[48] J. Wu, W.L. Nyborg, Ultrasound, cavitation bubbles and their interaction with cells, Adv. Drug Deliv. Rev. 60 (2008) 1103–1116.

[49] S. Hernot, A.L. Klibanov, Microbubbles in ultrasound-triggered drug and gene delivery, Adv. Drug Deliv. Rev. 60 (2008) 1153–1166.

[50] A. Joshi, J. Raje, Sonicated transdermal drug transport, J. Control. Release 83 (2002) 13–22.

[51] P. Loverock, G. ter Haar, M.G. Ormerod, P.R. Imrie, The effect of ultrasound on the cytotoxicity of adriamycin, Br. J. Radiol. 63 (1990) 542–546.

[52] A.H. Saad, G.M. Hahn, Ultrasound enhanced drug toxicity on Chinese hamster ovary cells in vitro, Cancer Res. 49 (1989) 5931–5934.

[53] A.H. Saad, G.M. Hahn, Ultrasound-enhanced effects of adriamycin against murine tumors, Ultrasound Med. Biol. 18 (1992) 715–723.

[54] A.H. Saad, A.R. Williams, Effects of therapeutic ultrasound on clearance rate of blood borne colloidal particles in vivo, Br. J. Cancer Suppl. 5 (1982) 202–205.

[55] W.G. Pitt, Defining the role of ultrasound in drug delivery, Am. J. Drug Deliv. 1 (2003) 27–42.

[56] M. Kaviany, Some aspects of enhanced heat diffusion in fluids by oscillation, Int. J. Heat Mass Transfer 29 (1986) 2002–2006.

[57] J.R. Lattin, D.M. Belnap, W.G. Pitt, Formation of eLiposomes as a drug delivery vehicle, Colloids Surf. B: Biointerfaces 89 (2012) 93–100.

[58] J.R. Lattin, W.G. Pitt, D.M. Belnap, G.A. Husseini, Ultrasound-induced calcein release from eLiposomes, Ultrasound Med. Biol. 38 (2012) 2163–2173.

[59] M. Javadi, W.G. Pitt, D.M. Belnap, N.H. Tsosie, J.M. Hartley, Encapsulating nanoemulsions inside eLiposomes for ultrasonic drug delivery, Langmuir 28 (2012) 14720–14729.

[60] M. Javadi, W.G. Pitt, C.M. Tracy, J.R. Barrow, B.M. Willardson, J.M. Hartley, N.H. Tsosie, Ultrasonic gene and drug delivery using eLiposomes, J. Control. Release 167 (2013) 92–100.

[61] S.B. Barnett, H.D. Rott, G.R. ter Haar, M.C. Ziskin, K. Maeda, The sensitivity of biological tissue to ultrasound, Ultrasound Med. Biol. 23 (1997) 805–812.

[62] S.B. Barnett, G.R. ter Haar, M.C. Ziskin, W.L. Nyborg, K. Maeda, J. Bang, Current status of research on biophysical effects of ultrasound, Ultrasound Med. Biol. 20 (1994) 205–218.

[63] M.C. Ziskin, S.B. Barnett, Ultrasound and the developing central nervous system, Ultrasound Med. Biol. 27 (2001) 875–876.

[64] D.M. Hallow, A.D. Mahajan, M.R. Prausnitz, Ultrasonically targeted delivery into endothelial and smooth muscle cells in ex vivo arteries, J. Controlled Release 118 (2007) 285–293.

[65] S. Meairs, A. Alonso, Ultrasound, microbubbles and the blood-brain barrier, Prog. Biophys. Mol. Biol. 93 (2007) 354–362.

[66] M.R. Bohmer, C.H. Chlon, B.I. Raju, C.T. Chin, T. Shevchenko, A.L. Klibanov, Focused ultrasound and microbubbles for enhanced extravasation, J. Control. Release 148 (2010) 18–24.

[67] G.A. Husseini, W.G. Pitt, Micelles and nanoparticles for ultrasonic drug and gene delivery, Adv. Drug Deliv. Rev. 60 (2008) 1137–1152.

[68] W.A.J. Howard, A. Bayomi, E. Natarajan, M.A.E.-A.O. Aziza, C.B. Grissom, F.G. West, Sonolysis promotes indirect Co C bond cleavage of alkylcob(III)alamin bioconjugates, Bioconjug. Chem. 8 (1997) 498–502.

[69] C.C. Coussios, C.K. Holland, L. Jakubowska, S.L. Huang, R.C. MacDonald, A. Nagaraj, D.D. McPherson, In vitro characterization of liposomes and Optison by acoustic scattering at 3.5 MHz, Ultrasound Med. Biol. 30 (2004) 181–190.

[70] S.L. Huang, Liposomes in ultrasonic drug and gene delivery, Adv. Drug Deliv. Rev. 60 (2008) 1167–1176.

[71] C.O. Rangel-Yagui, A. Pessoa Jr., L.C. Tavares, Micellar solubilization of drugs, J. Pharm. Pharm. Sci. 8 (2005) 147–165.

[72] G.A. Husseini, W.G. Pitt, The use of ultrasound and micelles in cancer treatment, J. Nanosci. Nanotechnol. 8 (2008) 2205–2215.

[73] H.M. Aliabadi, A. Lavasanifar, Polymeric micelles for drug delivery, Expert Opin. Drug Deliv. 3 (2006) 139–162.

[74] G. Gaucher, M.H. Dufresne, V.P. Sant, N. Kang, D. Maysinger, J.C. Leroux, Block copolymer micelles: preparation, characterization and application in drug delivery, J. Control. Release 109 (2005) 169–188.

[75] C. Oerlemans, W. Bult, M. Bos, G. Storm, J.F. Nijsen, W.E. Hennink, Polymeric micelles in anticancer therapy: targeting, imaging and triggered release, Pharm. Res. 27 (2010) 2569–2589.

[76] M.L. Adams, A. Lavasanifar, G.S. Kwon, Amphiphilic block copolymers for drug delivery, J. Pharm. Sci. 92 (2003) 1343–1355.

[77] P. Alexandridis, V. Athanassiou, T.A. Hatton, Pluronic-P105 PEO–PPO–PEO block copolymer in aqueous urea solutions: micelle formation, structure, and microenvironment, Langmuir 11 (1995) 2442–2450.

[78] P. Alexandridis, T.A. Hatton, Poly(ethyleneoxide)-poly(propyleneoxide)Poly(ethyleneoxide) block copolymer surfactants in aqueous solutions and at interfaces: thermodynamics, structure, dynamics, and modeling, Colloids Surf. A: Physicochem. Eng. Asp. 96 (1995) 1–46.

[79] P. Alexandridis, J.F. Holzwarth, T.A. Hatton, Micellization of poly(ethylene oxide)-poly(propylene oxide)-poly(ethylene oxide) triblock copolymer in aqueous solutions: thermodynamics of copolymer association, Macromolecules 27 (1994) 2414–2425.

[80] P. Alexandridis, T. Nivaggioli, T.A. Hatton, Temperature effects on structural properties of Pluronic P104 and F108 PEO–PPO–PEO block copolymer solutions, Langmuir 11 (1995) 1468–1476.

[81] N. Rapoport, K. Caldwell, Structural transitions in micellar solutions of Pluronic P-105 and their effect on the

conformation of dissolved cytochrome C: an electron paramagnetic resonance investigation, Colloids Surf. B: Biointerfaces 3 (1994) 217–228.

[82] N.Y. Rapoport, D.A. Christensen, H.D. Fain, L. Barrows, Z. Gao, Ultrasoundtriggered drug targeting of tumors in vitro and in vivo, Ultrasonics 42 (2004) 943–950.

[83] E.V. Batrakova, A.V. Kabanov, Pluronic block copolymers: evolution of drug delivery concept from inert nanocarriers to biological response modifiers, J. Control. Release 130 (2008) 98–106.

[84] G.A. Husseini, N.Y. Rapoport, D.A.P.J.D. Christensen, W.G. Pitt, Kinetics of ultrasonic release of doxorubicin from Pluronic P105 micelles, Colloids Surf. B: Biointerfaces 24 (2002) 253.

[85] N. Munshi, N. Rapoport, W.G. Pitt, Ultrasonic activated drug delivery from Pluronic P-105 micelles, Cancer Lett. 118 (1997) 13–19.

[86] N.Y. Rapoport, J.N. Herron, W.G. Pitt, L. Pitina, Micellar delivery of doxorubicin and its paramagnetic analog, ruboxyl, to HL-60 cells: effect of micelle structure and ultrasound on the intracellular drug uptake, J. Control. Release 58 (1999) 153–162.

[87] N. Rapoport, W.G. Pitt, H. Sun, J.L. Nelson, Drug delivery in polymeric micelles: from in vitro to in vivo, J. Control. Release 91 (2003) 85–95.

[88] J.D. Pruitt, G. Husseini, N. Rapoport, W.G. Pitt, Stabilization of Pluronic p-105 micelles with an interpenetrating network of n,n-diethylacrylamide, Macromolecules 33 (2000) 9306–9309.

[89] J.E. Chung, M. Yokoyama, M. Yamato, T. Aoyagi, Y. Sakurai, T. Okano, Thermoresponsive drug delivery from polymeric micelles constructed using block copolymers of poly(N-isopropylacrylamide) and poly(butylmethacrylate), J. Control. Release 62 (1999) 115–127.

[90] K. Kataoka, G.S. Kwon, M. Yokoyama, T. Okano, Y. Sakurai, Block copolymer micelles as vehicles for drug delivery, J. Control. Release 24 (1993) 119–132.

[91] K. Kataoka, T. Matsumoto, M. Yokoyama, T. Okano, Y. Sakurai, S. Fukushima, K. Okamoto, G.S. Kwon, Doxorubicin-loaded poly(ethylene glycol)-poly(beta-benzyl-l-aspartate) copolymer micelles: their pharmaceutical characteristics and biological significance, J. Control. Release 64 (2000) 143–153.

[92] G. Kwon, M. Naito, M. Yokoyama, T. Okano, Y. Sakurai, K. Kataoka, Micelles based on AB block copolymers of poly(ethylene oxide) and poly(.beta.-benzyl l-aspartate), Langmuir 9 (1993) 945–949.

[93] G. Kwon, M. Naito, M. Yokoyama, T. Okano, Y. Sakurai, K. Kataoka, Block copolymer micelles for drug delivery: loading and release of doxorubicin, J. Controlled Release 48 (1997) 195.

[94] G. Kwon, S. Suwa, M. Yokoyama, T. Okano, Y. Sakurai, K. Kataoka, Enhanced tumor accumulation and prolonged circulation times of micelle-forming poly (ethylene oxide-aspartate) block copolymer-adriamycin conjugates, J. Control. Release 29 (1994) 17–23.

[95] G.S. Kwon, M. Naito, K. Kataoka, M. Yokoyama, Y. Sakurai, T. Okano, Block copolymer micelles as vehicles for hydrophobic drugs, Colloids Surf. B: Biointerfaces 2 (1994) 429–434.

[96] G.S. Kwon, M. Naito, M. Yokoyama, T. Okano, Y. Sakurai, K. Kataoka, Physical entrapment of adriamycin in AB block copolymer micelles, Pharm. Res. 12 (1995) 192–195.

[97] G.S. Kwon, M. Yokoyama, T. Okano, Y. Sakurai, K. Kataoka, Biodistribution of micelle-forming polymer–drug conjugates, Pharm. Res. 10 (1993) 970–974.

[98] M. Yokoyama, G.S. Kwon, T. Okano, Y. Sakurai, T. Seto, K. Kataoka, Preparation of micelle-forming polymer–drug conjugates, Bioconjug. Chem. 3 (1992) 295–301.

[99] M. Yokoyama, T. Okano, Y. Sakurai, H. Ekimoto, C. Shibazaki, K. Kataoka, Toxicity and antitumor activity against solid tumors of micelle-forming polymeric anticancer drug and its extremely long circulation in blood, Cancer Res. 51 (1991) 3229–3236.

[100] M. Yokoyama, T. Okano, Y. Sakurai, S. Fukushima, K. Okamoto, K. Kataoka, Selective delivery of adriamycin to a solid tumor using a polymeric micelle carrier system, J. Drug Target. 7 (1999) 171–186.

[101] M. Yokoyama, T. Sugiyama, T. Okano, Y. Sakurai, M. Naito, K. Kataoka, Analysis of micelle formation of an adriamycin-conjugated poly(ethylene glycol)poly(aspartic acid) block copolymer by gel permeation chromatography, Pharm. Res. 10 (1993) 895–899.

[102] A.V. Kabanov, E.V. Batrakova, N.S. Melik-Nubarov, N.A. Fedoseev, T.Y. Dorodnich, V.Y. Alakhov, I.R. Nazarova, V.A. Kabanov, A new class of drug carriers: micelles of poly(oxyethylene)-poly(oxypropylene) block copolymers as microcontainers for targeting drugs from blood to brain, J. Control. Release 22 (1992) 141–158.

[103] N. Rapoport, L. Pitina, Intracellular distribution and intracellular dynamics of a spin-labeled analogue of doxorubicin fluorescence and EPR spectroscopy, J. Pharm. Sci. 87 (1998) 321–325.

[104] V. Alakhov, E. Moskaleva, E.V. Batrakova, A.V. Kabanov, Hypersensitization of multidrug resistant human ovarian carcinoma cells by Pluronic P85 block copolymer, Bioconjug. Chem. 7 (1996) 209–216.

[105] E. Batrakova, S. Li, S. Li, A. Venne, V. Alakhov, A. Kabanov, Fundamental relationships between the composition of Pluronic block copolymers and their hypersensitization effect in MDR cancer cells, Pharm. Res. 16 (1999) 1373–1379.

[106] A. Venne, S. Li, R. Mandeville, A. Kabanov, V. Alakhov, Hypersensitizing effect of Pluronic L61 on cytotoxic activity, transport, and subcellular distribution of

doxorubicin in multiple drug-resistant cells, Cancer Res. 56 (1996) 3626–3629.

[107] A. Mahmud, X.B. Xiong, H.M. Aliabadi, A. Lavasanifar, Polymeric micelles for drug targeting, J. Drug Target. 15 (2007) 553–584.

[108] A.V. Kabanov, V.P. Chekhonin, V. Alakhov, E.V. Batrakova, A.S. Lebedev, N.S. Melik-Nubarov, S.A. Arzhakov, A.V. Levashov, G.V. Morozov, E.S. Severin, et al., The neuroleptic activity of haloperidol increases after its solubilization in surfactant micelles. Micelles as microcontainers for drug targeting, FEBS Lett. 258 (1989) 343–345.

[109] V. Torchilin, Multifunctional and stimuli-sensitive pharmaceutical nanocarriers, Eur. J. Pharm. Biopharm. 71 (2009) 431–444.

[110] V.P. Torchilin, Micellar nanocarriers: pharmaceutical perspectives, Pharm. Res. 24 (2007) 1–16.

[111] C.P. Leamon, J.A. Reddy, Folate-targeted chemotherapy, Adv. Drug Deliv. Rev. 56 (2004) 1127–1141.

[112] N. Rapoport, Physical stimuli-responsive polymeric micelles for anti-cancer drug delivery, Prog. Polym. Sci. 32 (2007) 962–990.

[113] D. Kim, Z.G. Gao, E.S. Lee, Y.H. Bae, In vivo evaluation of doxorubicin-loaded polymeric micelles targeting folate receptors and early endosomal pH in drugresistant ovarian cancer, Mol. Pharmacol. 6 (2009) 1353–1362.

[114] E.S. Lee, Z. Gao, D. Kim, K. Park, I.C. Kwon, Y.H. Bae, Super pH-sensitive multifunctional polymeric micelle for tumor pH(e) specific TAT exposure and multidrug resistance, J. Control. Release 129 (2008) 228–236.

[115] V.A. Sethuraman, Y.H. Bae, TAT peptide-based micelle system for potential active targeting of anti-cancer agents to acidic solid tumors, J. Control. Release 118 (2007) 216–224.

[116] X.L. Wu, J.H. Kim, H. Koo, S.M. Bae, H. Shin, M.S. Kim, B.H. Lee, R.W. Park, I.S. Kim, K. Choi, I.C. Kwon, K. Kim, D.S. Lee, Tumor-targeting peptide conjugated pH-responsive micelles as a potential drug carrier for cancer therapy, Bioconjug. Chem. 21 (2010) 208–213.

[117] X. Yang, J.J. Grailer, S. Pilla, D.A. Steeber, S. Gong, Tumor-targeting, pHresponsive, and stable unimolecular micelles as drug nanocarriers for targeted cancer therapy, Bioconjug. Chem. 21 (2010) 496–504.

[118] G.A. Husseini, D. Velluto, L. Kherbeck, W.G. Pitt, J.A. Hubbell, D.A. Christensen, Investigating the acoustic release of doxorubicin from targeted micelles, Colloids Surf. B: Biointerfaces 101 (2012) 153–155.

[119] N. Rapoport, Combined cancer therapy by micellar-encapsulated drug and ultrasound, Int. J. Pharm. 277 (2004) 155–162.

[120] S. Martins, B. Sarmento, D.C. Ferreira, E.B. Souto, Lipid-based colloidal carriers for peptide and protein delivery – liposomes versus lipid nanoparticles, Int. J. Nanomed. 2 (2007) 595–607.

[121] M. Rawat, D. Singh, S. Saraf, Nanocarriers: promising vehicle for bioactive drugs, Biol. Pharm. Bull. 29 (2006) 1790–1798.

[122] G. Gregoriades, A.T. Florence, H.M. Patel, Liposomes in Drug Delivery, Harwood Academic Publishers, Amsterdam, 1993.

[123] V.V. Kumar, Complementary molecular shapes and additivity of the packing parameter of lipids, Proc. Natl. Acad. Sci. U. S. A. 88 (1991) 444–448.

[124] D. Lichtenberg, Y. Barenholz, Liposomes: preparation, characterization, and preservation, Methods Biochem. Anal. 33 (1988) 337–462.

[125] Y. Barenholz, D. Gibbes, B.J. Litman, J. Goll, T.E. Thompson, R.D. Carlson, A simple method for the preparation of homogeneous phospholipid vesicles, Biochemistry 16 (1977) 2806–2810.

[126] C. Huang, Studies on phosphatidylcholine vesicles. Formation and physical characteristics, Biochemistry 8 (1969) 344–352.

[127] C. Huang, Carriers and specificity in membranes. IV. Model vesicles and membranes. Phosphatidylcholine vesicles: formation, physical characteristics and dye-lipid interaction, Neurosci. Res. Program Bull. 9 (1971) 380–381.

[128] M.J. Hope, M.B. Bally, G. Webb, P.R. Cullis, Production of large unilamellar vesicles by a rapid extrusion procedure: characterization of size distribution, trapped volume and ability to maintain a membrane potential, Biochim. Biophys. Acta 812 (1985) 55–65.

[129] A. Schroeder, J. Kost, Y. Barenholz, Ultrasound, liposomes, and drug delivery: principles for using ultrasound to control the release of drugs from liposomes, Chem. Phys. Lipids 162 (2009) 1–16.

[130] Y. Barenholz, Cholesterol and other membrane active sterols: from membrane evolution to rafts, Prog. Lipid Res. 41 (2002) 1–5.

[131] K. Jorgensen, O.G. Mouritsen, Phase separation dynamics and lateral organization of two-component lipid membranes, Biophys. J. 69 (1995) 942–954.

[132] M.B. Yatvin, J.N. Weinstein, W.H. Dennis, R. Blumenthal, Design of liposomes for enhanced local release of drugs by hyperthermia, Science 202 (1978) 1290–1293.

[133] Y. Barenholz, G. Cevc, Structure and Properties of Membranes in Physical Chemistry of Biological Surfaces, Marcel Dekker, New York, 2000.

[134] T. Ta, T.M. Porter, Thermosensitive liposomes for localized delivery and triggered release of chemotherapy, J. Control. Release 169 (2013) 112–125.

[135] U. Boas, P.M. Heegaard, Dendrimers in drug research, Chem. Soc. Rev. 33 (2004) 43–63.

[136] W.H. De Jong, P.J. Borm, Drug delivery and nanoparticles:applications and hazards, Int. J. Nanomed. 3 (2008) 133–149.

[137] O.V. Chumakova, A.V. Liopo, V.G. Andreev, I. Cicenaite, B.M. Evers, S. Chakrabarty, T.C. Pappas, R.O. Esenaliev, Composition of PLGA and PEI/DNA nanoparticles improves ultrasound-mediated gene delivery in solid tumors in vivo, Cancer Lett. 261 (2008) 215–225.

[138] M. Figueiredo, R. Esenaliev, PLGA nanoparticles for ultrasound-mediated gene delivery to solid tumors, J. Drug Deliv. 2012 (2012) 767839.

[139] P. Kohli, C.R. Martin, Smart nanotubes for biotechnology, Curr. Pharm. Biotechnol. 6 (2005) 35–47.

[140] M.J. Tiera, F.O. Winnik, J.C. Fernandes, Synthetic and natural polycations for gene therapy: state of the art and new perspectives, Curr. Gene Ther. 6 (2006) 59–71.

[141] M. Campone, J.M. Rademaker-Lakhai, J. Bennouna, S.B. Howell, D.P. Nowotnik, J.H. Beijnen, J.H.M. Schellens, Phase I and pharmacokinetic trial of AP5346, a DACH-platinum-polymer conjugate, administered weekly for three out of every 4 weeks to advanced solid tumor patients, Cancer Chemother. Pharmacol. 60 (2007) 523–533.

[142] S. Wang, J.B. Mi, Y.Z. Li, W.B. Chang, Y.X. Ci, M.Z. Zhao, Y.K. Zhao, L.Y. Zhu, G. Xu, Pharmacokinetics and tissue distribution of IV injection of polyphase liposome-encapsulated cisplatin (KM-1) in rats, Acta Pharmacol. Sin. 24 (2003) 589–592.

[143] E.V. Batrakova, T.Y. Dorodnych, E.Y. Klinskii, E.N. Kliushnenkova, O.B. Shemchukova, O.N. Goncharova, S.A. Arjakov, V.Y. Alakhov, A.V. Kabanov, Anthracycline antibiotics non-covalently incorporated into the block copolymer micelles: in vivo evaluation of anti-cancer activity, Br. J. Cancer 74 (1996) 1545–1552.

[144] M.A. Diaz-De-La-Rosa, High-Frequency Ultrasound Drug Delivery and Cavitation (M.Sc. Thesis), Brigham Young University, Provo, UT, 2007.

[145] G.A. Husseini, N.M. Abdel-Jabbar, F.S. Mjalli, W.G. Pitt, Modeling and sensitivity analysis of acoustic release of doxorubicin from unstabilized Pluronic P105 using an artificial neural network model, Technol. Cancer Res. Treat. 6 (2007) 49–56.

[146] G.A. Husseini, M.A.D. de la Rosa, E.O. AlAqqad, S. Al Mamary, Y. Kadimati, A. Al Baik, W.G. Pitt, Kinetics of acoustic release of doxorubicin from stabilized and unstabilized micelles and the effect of temperature, J. Franklin Inst. 348 (2011) 125.

[147] G.A. Husseini, M.A. Diaz de la Rosa, T. Gabuji, Y. Zeng, D.A. Christensen, W.G. Pitt, Release of doxorubicin from unstabilized and stabilized micelles under the action of ultrasound, J. Nanosci. Nanotechnol. 7 (2007) 1028–1033.

[148] Y. Zeng, W.G. Pitt, Poly(ethylene oxide)-b-poly(n-isopropylacrylamide) nanoparticles with crosslinked cores as drug carriers, J. Biomater. Sci. Polym. 16 (2005) 371–380.

[149] Y. Zeng, W.G. Pitt, A polymeric micelle system with a hydrolysable segment for drug delivery, J. Biomater. Sci. Polym. Ed. 17 (2006) 591–604.

[150] B. Howard, A. Gao, S.-W. Lee, M.-H. Seo, N. Rapoport, Ultrasoundenhanced chemotherapy of drug-resistant breast cancer tumors by micellar-encapsulated paclitaxel, Am. J. Drug Deliv. 4 (2006) 97–104.

[151] N. Rapoport, A.P. Marin, A.A. Timoshin, Effect of a polymeric surfactant on electron transport in HL-60 cells, Arch. Biochem. Biophys. 384 (2000) 100–108.

[152] N. Rapoport, A.I. Smirnov, W.G. Pitt, A.A. Timoshin, Bioreduction of tempone and spin-labeled gentamicin by gram-negative bacteria: kinetics and effect of ultrasound, Arch. Biochem. Biophys. 362 (1999) 233–241.

[153] K. Dorn, G. Hoerpel, H. Ringsdorf, Polymeric anti-tumor agents on a molecular and cellular level, in: C.G. Gebelein, C.E. Carraher Jr. (Eds.), Bioactive Polymeric Systems, Plenum, New York, 1985, pp. 531–585.

[154] A.V. Kabanov, E.V. Batrakova, V.Y. Alakhov, Pluronic block copolymers for overcoming drug resistance in cancer, Adv. Drug Deliv. Rev. 54 (2002) 759–779.

[155] E.V. Batrakova, S. Li, W.F. Elmquist, D.W. Miller, V.Y. Alakhov, A.V. Kabanov, Mechanism of sensitization of MDR cancer cells by Pluronic block copolymers: selective energy depletion, Br. J. Cancer 85 (2001) 1987–1997.

[156] W. Hong, D. Chen, X. Zhang, J. Zeng, H. Hu, X. Zhao, M. Qiao, Reversing multidrug resistance by intracellular delivery of Pluronic(R) P85 unimers, Biomaterials 34 (2013) 9602–9614.

[157] G.A. Husseini, D.A. Christensen, N.Y. Rapoport, W.G. Pitt, Ultrasonic release of doxorubicin from Pluronic P105 micelles stabilized with an interpenetrating network of N,N-diethylacrylamide, J. Control. Release 83 (2002) 303–305.

[158] Z. Gao, H.D. Fain, N. Rapoport, Ultrasound-enhanced tumor targeting of polymeric micellar drug carriers, Mol. Pharmacol. 1 (2004) 317–330.

[159] Z.G. Gao, H.D. Fain, N. Rapoport, Controlled and targeted tumor chemotherapy by micellar-encapsulated drug and ultrasound, J. Control. Release 102 (2005) 203–222.

[160] T.T. Beaudette, J.A. Cohen, E.M. Bachelder, K.E. Broaders, J.L. Cohen, E.G. Engleman, J.M. Frechet, Chemoselective ligation in the functionalization of polysaccharide-based particles, J. Am. Chem. Soc. 131 (2009) 10360–10361.

[161] S. Boonyarattanakalin, J. Hu, S.A. Dykstra-Rummel, A. August, B.R. Peterson, Endocytic delivery of vancomycin mediated by a synthetic cell surface receptor: rescue of bacterially infected Mammalian cells and tissue targeting in vivo, J. Am. Chem. Soc. 129 (2007) 268–269.

[162] O. Nakagawa, X. Ming, L. Huang, R.L. Juliano, Targeted intracellular delivery of antisense oligonucleotides via

conjugation with small-molecule ligands, J. Am. Chem. Soc. 132 (2010) 8848–8849.

[163] R. Battino, T.R. Rettich, T. Tominaga, The solubility of nitrogen and air in liquids, J. Phys. Chem. Ref. Data 13 (1984) 563.

[164] U. Parlitz, V. Englisch, C. Scheffczyk, W. Lauterborn, Bifurcation structure of bubble oscillators, J. Acoust. Soc. Am. 88 (1990) 1061–1077.

[165] M.A. Diaz de la Rosa, G.A. Husseini, W.G. Pitt, Comparing microbubble cavitation at 500 kHz and 70 kHz related to micellar drug delivery using ultrasound, Ultrasonics 53 (2013) 377–386.

[166] M.A. Diaz de la Rosa, G.A. Husseini, W.G. Pitt, Mathematical modeling of microbubble cavitation at 70 kHz and the importance of the subharmonic in drug delivery from micelles, Ultrasonics 53 (2013) 97–110.

[167] D. Stevenson-Abouelnasr, G.A. Husseini, W.G. Pitt, Further investigation of the mechanism of doxorubicin release from P105 micelles using kinetic models, Colloids Surf. B: Biointerfaces 55 (2007) 59–66.

[168] G.A. Husseini, D. Stevenson-Abouelnasr, W.G. Pitt, K.T. Assaleh, L.O. Farahat, J. Fahadi, Kinetics and thermodynamics of acoustic release of doxorubicin from non-stabilized polymeric micelles, Colloids Surf. A: Physicochem. Eng. Asp. 359 (2010) 18–24.

[169] G.A. Husseini, N.M. Abdel-Jabbar, F.S. Mjalli, W.G. Pitt, A. Al-Mousa, Optimizing the use of ultrasound to deliver chemotherapeutic agents to cancer cells from polymeric micelles, J. Franklin Inst. 348 (2011) 1276–1284.

[170] G.A. Husseini, F.S. Mjalli, W.G. Pitt, N. Abdel-Jabbar, Using artificial neural networks and model predictive control to optimize acoustically assisted doxorubicin release from polymeric micelles, Technol. Cancer Res. Treat. 8 (2009) 479–488.

[171] H. Zhang, H. Xia, J. Wang, Y. Li, High intensity focused ultrasound-responsive release behavior of PLA-b-PEG copolymer micelles, J. Control. Release 139 (2009) 31–39.

[172] J. Wang, M. Pelletier, H. Zhang, H. Xia, Y. Zhao, High-frequency ultrasoundresponsive block copolymer micelle, Langmuir 25 (2009) 13201–13205.

[173] G.A. Husseini, K.L. O'Neill, W.G. Pitt, The comet assay to determine the mode of cell death for the ultrasonic delivery of doxorubicin to human leukemia (HL60 Cells) from Pluronic P105 micelles, Technol. Cancer Res. Treat. 4 (2005) 707–711.

[174] J.D. Pruitt, W.G. Pitt, Sequestration and ultrasound-induced release of doxorubicin from stabilized Pluronic P105 micelles, Drug Deliv. 9 (2002) 253–258.

[175] A. Marin, M. Muniruzzaman, N. Rapoport, Mechanism of the ultrasonic activation of micellar drug delivery, J. Control. Release 75 (2001) 69–81.

[176] A. Marin, M. Muniruzzaman, N. Rapoport, Acoustic activation of drug delivery from polymeric micelles: effect of pulsed ultrasound, J. Control. Release 71 (2001) 239–249.

[177] N. Rapoport, A. Marin, Y. Luo, G.D. Prestwich, M.D. Muniruzzaman, Intracellular uptake and trafficking of Pluronic micelles in drug-sensitive and MDR cells: effect on the intracellular drug localization, J. Pharm. Sci. 91 (2002) 157–170.

[178] G.A. Husseini, C.M. Runyan, W.G. Pitt, Investigating the mechanism of acoustically activated uptake of drugs from Pluronic micelles, BMC Cancer 2 (2002) 20.

[179] H.J. Lin, P. Herman, J.S. Kang, J.R. Lakowicz, Fluorescence lifetime characterization of novel low-pH probes, Anal. Biochem. 294 (2001) 118–125.

[180] N. Sheikov, N. McDannold, F. Jolesz, Y.Z. Zhang, K. Tam, K. Hynynen, Brain arterioles show more active vesicular transport of blood-borne tracer molecules than capillaries and venules after focused ultrasound-evoked opening of the blood-brain barrier, Ultrasound Med. Biol. 32 (2006) 1399–1409.

[181] B.D. Meijering, L.J. Juffermans, A. van Wamel, R.H. Henning, I.S. Zuhorn, M. Emmer, A.M. Versteilen, W.J. Paulus, W.H. van Gilst, K. Kooiman, N. de Jong, R.J. Musters, L.E. Deelman, O. Kamp, Ultrasound and microbubble-targeted delivery of macromolecules is regulated by induction of endocytosis and pore formation, Circ. Res. 104 (2009) 679–687.

[182] J. Hauser, M. Ellisman, H.U. Steinau, E. Stefan, M. Dudda, M. Hauser, Ultrasound enhanced endocytotic activity of human fibroblasts, Ultrasound Med. Biol. 35 (2009) 2084–2092.

[183] P. Prentice, A. Cuschierp, K. Dholakia, M. Prausnitz, P. Campbell, Membrane disruption by optically controlled microbubble cavitation, Nat. Phys. 1 (2005) 107–110.

[184] R.K. Schlicher, J.D. Hutcheson, H. Radhakrishna, R.P. Apkarian, M.R. Prausnitz, Changes in cell morphology due to plasma membrane wounding by acoustic cavitation, Ultrasound Med. Biol. 36 (2010) 677–692.

[185] A. van Wamel, K. Kooiman, M. Harteveld, M. Emmer, F.J. ten Cate, M. Versluis, N. de Jong, Vibrating microbubbles poking individual cells: drug transfer into cells via sonoporation, J. Control. Release 112 (2006) 149–155.

[186] Y. Zhou, R.E. Kumon, J. Cui, C.X. Deng, The size of sonoporation pores on the cell membrane, Ultrasound Med. Biol. 35 (2009) 1756–1760.

[187] S.B. Stringham, B.K. Murray, K.L. O'Neill, S. Ohmine, T.A. Gaufin, W.G. Pitt, Mechanism of targeted chemotherapeutic delivery using ultrasound, in: 96th Annual Meeting of the American Association for Cancer Research, Anaheim, CA, USA, 2005.

[188] M.R. Bailey, L.N. Couret, O.A. Sapozhnikov, V.A. Khokhlova, G. ter Haar, S. Vaezy, X. Shi, R. Martin, L.A. Crum, Use of overpressure to assess the role of bubbles in

focused ultrasound lesion shape in vitro, Ultrasound Med. Biol. 27 (2001) 695–708.

[189] E.S. Richardson, W.G. Pitt, D.J. Woodbury, The role of cavitation in liposome formation, Biophys. J. 93 (2007) 4100–4107.

[190] M. Ugarenko, C.K. Chan, A. Nudelman, A. Rephaeli, S.M. Cutts, D.R. Phillips, Development of Pluronic micelle-encapsulated doxorubicin and formaldehyde-releasing prodrugs for localized anticancer chemotherapy, Oncol. Res. 17 (2009) 283–299.

[191] L. Chen, X. Sha, X. Jiang, Y. Chen, Q. Ren, X. Fang, Pluronic P105/F127 mixed micelles for the delivery of docetaxel against Taxol-resistant non-small cell lung cancer: optimization and in vitro, in vivo evaluation, Int. J. Nanomed. 8 (2013) 73–84.

[192] Z.G. Gao, D.H. Lee, D.I. Kim, Y.H. Bae, Doxorubicin loaded pH-sensitive micelle targeting acidic extracellular pH of human ovarian A2780 tumor in mice, J. Drug Target. 13 (2005) 391–397.

[193] N. Rapoport, Z. Gao, A. Kennedy, Multifunctional nanoparticles for combining ultrasonic tumor imaging and targeted chemotherapy, J. Natl. Cancer Inst. 99 (2007) 1095–1106.

[194] G. Myhr, J. Moan, Synergistic and tumour selective effects of chemotherapy and ultrasound treatment, Cancer Lett. 232 (2006) 206–213.

[195] J.L. Nelson, Ultrasonically Enhanced Drug Delivery of Doxorubicin In Vivo from Stabilized Pluronic Micelle Carriers (M.Sc. thesis), Brigham Young University, Provo, UT, 2002.

[196] J.L. Nelson, B.L. Roeder, J.C. Carmen, F. Roloff, W.G. Pitt, Ultrasonically activated chemotherapeutic drug delivery in a rat model, Cancer Res. 62 (2002) 7280–7283.

[197] B.J. Staples, Pharmacokinetics of Ultrasonically-Released, MicelleEncapsulated Doxorubicin in the Rat Model and Its Effect on Tumor Growth (M.Sc. thesis), Brigham Young University, Provo, UT, 2007.

[198] B.J. Staples, B.L. Roeder, G.A. Husseini, O. Badamjav, G.B. Schaalje, W.G. Pitt, Role of frequency and mechanical index in ultrasonic-enhanced chemotherapy in rats, Cancer Chemother. Pharmacol. 64 (2009) 593–600.

[199] B.J. Staples, W.G. Pitt, B.L. Roeder, G.A. Husseini, D. Rajeev, G.B. Schaalje, Distribution of doxorubicin in rats undergoing ultrasonic drug delivery, J. Pharm. Sci. 99 (2010) 3122–3131.

[200] B.J. Staples, B.L. Roeder, W.G. Pitt, Annual Meeting of the Society for Biomaterials, Pittsburgh, PA, USA, 2006, 476 pp.

[201] R.T. Chlebowski, Adriamycin (doxorubicin) cardiotoxicity: a review, West. J. Med. 131 (1979) 364–368.

[202] H. Hasanzadeh, M. Mokhtari-Dizaji, S.Z. Bathaie, Z.M. Hassan, Effect of local dual frequency sonication on drug distribution from polymeric nanomicelles, Ultrason. Sonochem. 18 (2011) 1165–1171.

[203] C.Y. Lin, T.M. Liu, C.Y. Chen, Y.L. Huang, W.K. Huang, C.K. Sun, F.H. Chang, W.L. Lin, Quantitative and qualitative investigation into the impact of focused ultrasound with microbubbles on the triggered release of nanoparticles from vasculature in mouse tumors, J. Control. Release 146 (2010) 291–298.

[204] S. Samuel, M.A. Cooper, J.L. Bull, J.B. Fowlkes, D.L. Miller, An ex vivo study of the correlation between acoustic emission and microvascular damage, Ultrasound Med. Biol. 35 (2009) 1574–1586.

[205] S.M. Stieger, C.F. Caskey, R.H. Adamson, S. Qin, F.R. Curry, E.R. Wisner, K.W. Ferrara, Enhancement of vascular permeability with low-frequency contrastenhanced ultrasound in the chorioallantoic membrane model, Radiology 243 (2007) 112–121.

[206] G.S. Kwon, M. Yokoyama, T. Okano, Y. Sakurai, K. Kataoka, Enhanced tumor accumulation and prolonged circulation times of micelle-forming poly(ethylene oxide-co-aspartate) block copolymer-adriamycin conjugates, in: 6th International Symposium on Recent Advantages in Drug Delivery Systems, Salt Lake City, UT, USA, 1993.

[207] K. Saito, K. Miyake, P.L. McNeil, K. Kato, K. Yago, N. Sugai, Plasma membrane disruption underlies injury of the corneal endothelium by ultrasound, Exp. Eye Res. 68 (1999) 431–437.

[208] K. Ogawa, K. Tachibana, T. Uchida, T. Tai, N. Yamashita, N. Tsujita, R. Miyauchi, High-resolution scanning electron microscopic evaluation of cell-membrane porosity by ultrasound, Med. Electron. Microsc. 34 (2001) 249–253.

[209] Y. Taniyama, K. Tachibana, K. Hiraoka, M. Aoki, S. Yamamoto, K. Matsumoto, T. Nakamura, T. Ogihara, Y. Kaneda, R. Morishita, Development of safe and efficient novel nonviral gene transfer using ultrasound: enhancement of transfection efficiency of naked plasmid DNA in skeletal muscle, Gene Ther. 9 (2002) 372–380.

[210] Y. Taniyama, K. Tachibana, K. Hiraoka, T. Namba, K. Yamasaki, N. Hashiya, M. Aoki, T. Ogihara, K. Yasufumi, R. Morishita, Local delivery of plasmid DNA into rat carotid artery using ultrasound, Circulation 105 (2002) 1233–1239.

[211] G.V. Betageri, S.A. Jenkins, D. Parsons, Liposome Drug Delivery Systems, Technomic, Lancaster, PA, 1993.

[212] P.P. Deshpande, S. Biswas, V.P. Torchilin, Current trends in the use of liposomes for tumor targeting, Nanomedicine (Lond.) 8 (2013) 1509–1528.

[213] M. Honda, T. Asai, N. Oku, Y. Araki, M. Tanaka, N. Ebihara, Liposomes and nanotechnology in drug development: focus on ocular targets, Int. J. Nanomed. 8 (2013) 495–503.

[214] H. Grull, S. Langereis, Hyperthermia-triggered drug delivery from temperature-sensitive liposomes using MRI-

guided high intensity focused ultrasound, J. Control. Release 161 (2012) 317–327.

[215] C.D. Landon, J.Y. Park, D. Needham, M.W. Dewhirst, Nanoscale drug delivery and hyperthermia: the materials design and preclinical and clinical testing of low temperature-sensitive liposomes used in combination with mild hyperthermia in the treatment of local cancer, Open Nanomed. J. 3 (2011) 38–64.

[216] S. Ferreira Ddos, S.C. Lopes, M.S. Franco, M.C. Oliveira, pH-sensitive liposomes for drug delivery in cancer treatment, Ther. Deliv. 4 (2013) 1099–1123.

[217] L.H. Lindner, M. Hossann, Factors affecting drug release from liposomes, Curr. Opin. Drug Discov. Dev. 13 (2010) 111–123.

[218] T.L. Andresen, D.H. Thompson, T. Kaasgaard, Enzyme-triggered nanomedicine: drug release strategies in cancer therapy, Mol. Membr. Biol. 27 (2010) 353–363.

[219] S.J. Leung, M. Romanowski, Light-activated content release from liposomes, Theranostics 2 (2012) 1020–1036.

[220] D. Qiu, X. An, Controllable release from magnetoliposomes by magnetic stimulation and thermal stimulation, Colloids Surf. B: Biointerfaces 104 (2013) 326–329.

[221] H. Ding, V. Sagar, M. Agudelo, S. Pilakka-Kanthikeel, V.S. Atluri, A. Raymond, T. Samikkannu, M.P. Nair, Enhanced blood-brain barrier transmigration using a novel transferrin embedded fluorescent magneto-liposome nanoformulation, Nanotechnology 25 (2014) 055101.

[222] T. Saxer, A. Zumbuehl, B. Muller, The use of shear stress for targeted drug delivery, Cardiovasc. Res. 99 (2013) 328–333.

[223] E.C. Unger, T.P. McCreery, R.H. Sweitzer, V.E. Caldwell, Y. Wu, Acoustically active lipospheres containing paclitaxel: a new therapeutic ultrasound contrast agent, Invest. Radiol. 33 (1998) 886–892.

[224] T. Yamashita, S. Sonoda, R. Suzuki, N. Arimura, K. Tachibana, K. Maruyama, T. Sakamoto, A novel bubble liposome and ultrasound-mediated gene transfer to ocular surface: RC-1 cells in vitro and conjunctiva in vivo, Exp. Eye Res. 85 (2007) 741–748.

[225] R. Suzuki, T. Takizawa, Y. Negishi, K. Hagisawa, K. Tanaka, K. Sawamura, N. Utoguchi, T. Nishioka, K. Maruyama, Gene delivery by combination of novel liposomal bubbles with perfluoropropane and ultrasound, J. Control. Release 117 (2007) 130–136.

[226] M. Javadi, H. Bingham, W.G. Pitt, Pactlitaxel delivery to tumor cells using eLiposomes and ultrasound, in preparation, 2014.

[227] X.Y. Xi, F. Yang, D. Chen, Y. Luo, D. Zhang, N. Gu, J.R. Wu, A targeting drugdelivery model via interactions among cells and liposomes under ultrasonic excitation, Phys. Med. Biol. 53 (2008) 3251–3265.

[228] K. Shiraishi, R. Endoh, H. Furuhata, M. Nishihara, R. Suzuki, K. Maruyama, Y. Oda, J. Jo, Y. Tabata, J. Yamamoto, M. Yokoyama, A facile preparation method of a PFC-containing nano-sized emulsion for theranostics of solid tumors, Int. J. Pharm. 421 (2011) 379–387.

[229] A. Kheirolomoom, P.A. Dayton, A.F.H. Lum, E. Little, E.E. Paoli, H. Zheng, K.W. Ferrara, Acoustically-active microbubbles conjugated to liposomes: characterization of a proposed drug delivery vehicle, J. Control. Release 118 (2007) 275–284.

[230] A.T. Nguyen, S.P. Wrenn, Acoustically active liposome-nanobubble complexes for enhanced ultrasonic imaging and ultrasound-triggered drug delivery, Wiley Interdiscip. Rev. Nanomed. Nanobiotechnol. 6 (2014) 316–325.

[231] S.M. Graham, R. Carlisle, J.J. Choi, M. Stevenson, A.R. Shah, R.S. Myers, K. Fisher, M.-B. Peregrino, L. Seymour, C.C. Coussios, Inertial cavitation to non-invasively trigger and monitor intratumoral release of drug from intravenously delivered liposomes, J. Controlled Release 178 (2014) 101–107.

[232] A. Yudina, M. de Smet, M. Lepetit-Coiffe, S. Langereis, L. Van Ruijssevelt, P. Smirnov, V. Bouchaud, P. Voisin, H. Grull, C.T. Moonen, Ultrasound-mediated intracellular drug delivery using microbubbles and temperature-sensitive liposomes, J. Control. Release 155 (2011) 442–448.

[233] S.M. Park, M.S. Kim, S.J. Park, E.S. Park, K.S. Choi, Y.S. Kim, H.R. Kim, Novel temperature-triggered liposome with high stability: formulation, in vitro evaluation, and in vivo study combined with high-intensity focused ultrasound (HIFU), J. Control. Release 170 (2013) 373–379.

[234] M. de Smet, S. Langereis, S. van den Bosch, K. Bitter, N.M. Hijnen, E. Heijman, H. Grull, SPECT/CT imaging of temperature-sensitive liposomes for MR-image guided drug delivery with high intensity focused ultrasound, J. Control. Release 169 (2013) 82–90.

[235] S. Ibsen, M. Benchimol, D. Simberg, C. Schutt, J. Steiner, S. Esener, A novel nested liposome drug delivery vehicle capable of ultrasound triggered release of its payload, J. Control. Release 155 (2011) 358–366.

[236] T. Yin, P. Wang, J. Li, R. Zheng, B. Zheng, D. Cheng, R. Li, J. Lai, X. Shuai, Ultrasound-sensitive siRNA-loaded nanobubbles formed by hetero-assembly of polymeric micelles and liposomes and their therapeutic effect in gliomas, Biomaterials 34 (2013) 4532–4543.

[237] R. Liu, X. Wei, Y. Yao, Q. Chai, Y. Chen, Y. Xu, The preparation and characterization of gas bubble containing liposomes, Conf. Proc. IEEE Eng. Med. Biol. Soc. 4 (2005) 3998–4001.

[238] M.F. Chung, K.J. Chen, H.F. Liang, Z.X. Liao, W.T. Chia, Y. Xia, H.W. Sung, A liposomal system capable of generating CO_2 bubbles to induce transient cavitation, lysosomal rupturing, and cell necrosis, Angew. Chem. Int. Ed. Engl. 51 (2012) 10089–10093.

[239] K.J. Chen, H.F. Liang, H.L. Chen, Y. Wang, P.Y. Cheng, H.L. Liu, Y. Xia, H.W. Sung, A thermoresponsive bubble-

generating liposomal system for triggering localized extracellular drug delivery, ACS Nano 7 (2013) 438–446.

[240] S.L. Huang, D.D. McPherson, R.C. Macdonald, A method to co-encapsulate gas and drugs in liposomes for ultrasound-controlled drug delivery, Ultrasound Med. Biol. 34 (2008) 1272–1280.

[241] S.L. Huang, A.J. Hamilton, E. Pozharski, A. Nagaraj, M.E. Klegerman, D.D. McPherson, R.C. MacDonald, Physical correlates of the ultrasonic reflectivity of lipid dispersions suitable as diagnostic contrast agents, Ultrasound Med. Biol. 28 (2002) 339–348.

[242] S.L. Huang, Ultrasound-responsive liposomes, Methods Mol. Biol. 605 (2010) 113–128.

[243] J.A. Kopechek, K.J. Haworth, K. Radhakrishnan, S.L. Huang, M.E. Klegerman, D.D. McPherson, C.K. Holland, The impact of bubbles on measurement of drug release from echogenic liposomes, Ultrason. Sonochem. 20 (2013) 1121–1130.

[244] P.H. Kee, T.A. Abruzzo, D.A. Smith, J.A. Kopechek, B. Wang, S.L. Huang, R.C. MacDonald, C.K. Holland, D.D. McPherson, Synthesis, acoustic stability, and pharmacologic activities of papaverine-loaded echogenic liposomes for ultrasound controlled drug delivery, J. Liposome Res. 18 (2008) 263–277.

[245] J.A. Kopechek, T.M. Abruzzo, B. Wang, S.M. Chrzanowski, D.A.B. Smith, P.H. Kee, S. Huang, J.H. Collier, D.D. McPherson, C.K. Holland, Ultrasound-mediated release of hydrophilic and lipophilic agents from echogenic liposomes, J. Ultrasound Med. 27 (2008) 1597–1606.

[246] J.A. Kopechek, K.J. Haworth, J.L. Raymond, T.D. Mast, S.R. Perrin, M.E. Klegerman, S.L. Huang, T.M. Porter, D.D. McPherson, C.K. Holland, Acoustic characterization of echogenic liposomes: frequency-dependent attenuation and backscatter, J. Acoust. Soc. Am. 130 (2011) 3472–3481.

[247] G.J. Shaw, J.M. Meunier, S.L. Huang, C.J. Lindsell, D.D. McPherson, C.K. Holland, Ultrasound-enhanced thrombolysis with tPA-loaded echogenic liposomes, Thromb. Res. 124 (2009) 306–310.

[248] K.D. Buchanan, S.L. Huang, H. Kim, D.D. McPherson, R.C. MacDonald, Encapsulation of NF-kappaB decoy oligonucleotides within echogenic liposomes and ultrasound-triggered release, J. Control. Release: Off. J. Control. Release Soc. 141 (2010) 193–198.

[249] Y.K. Luo, Y.Z. Zhao, C.T. Lu, J. Tang, X.K. Li, Application of ultrasonic gas-filled liposomes in enhancing transfer for breast cancer-related antisense oligonucleotides: an experimental study, J. Liposome Res. 18 (2008) 341–351.

[250] S.T. Laing, M.R. Moody, H. Kim, B. Smulevitz, S.L. Huang, C.K. Holland, D.D. McPherson, M.E. Klegerman, Thrombolytic efficacy of tissue plasminogen activator-loaded echogenic liposomes in a rabbit thrombus model, Thromb. Res. 130 (2012) 629–635.

[251] D.A.B. Smith, T.M. Porter, J. Martinez, S.L. Huang, R.C. MacDonald, D.D. McPherson, C.K. Holland, Destruction thresholds of echogenic liposomes with clinical diagnostic ultrasound, Ultrasound Med. Biol. 33 (2007) 797–809.

[252] R. Suzuki, Y. Oda, N. Utoguchi, K. Maruyama, Development of ultrasonic cancer therapy using ultrasound sensitive liposome, Yakugaku Zasshi. 130 (2010) 1665–1670.

[253] Y. Negishi, Y. Endo, T. Fukuyama, R. Suzuki, T. Takizawa, D. Omata, K. Maruyama, Y. Aramaki, Delivery of siRNA into the cytoplasm by liposomal bubbles and ultrasound, J. Control. Release 132 (2008) 124–130.

[254] R. Suzuki, E. Namai, Y. Oda, N. Nishiie, S. Otake, R. Koshima, K. Hirata, Y. Taira, N. Utoguchi, Y. Negishi, S. Nakagawa, K. Maruyama, Cancer gene therapy by IL12 gene delivery using liposomal bubbles and tumoral ultrasound exposure, J. Control. Release: Off. J. Control. Release Soc. 142 (2010) 245–250.

[255] R. Suzuki, T. Takizawa, Y. Negishi, N. Utoguchi, K. Maruyama, Effective gene delivery with novel liposomal bubbles and ultrasonic destruction technology, Int. J. Pharm. 354 (2008) 49–55.

[256] Y. Endo-Takahashi, Y. Negishi, A. Nakamura, S. Ukai, K. Ooaku, Y. Oda, K. Sugimoto, F. Moriyasu, N. Takagi, R. Suzuki, K. Maruyama, Y. Aramaki, Systemic delivery of miR-126 by miRNA-loaded Bubble liposomes for the treatment of hindlimb ischemia, Sci. Rep. 4 (2014) 3883.

[257] D. Omata, Y. Negishi, S. Hagiwara, S. Yamamura, Y. Endo-Takahashi, R. Suzuki, K. Maruyama, Y. Aramaki, Enhanced gene delivery using Bubble liposomes and ultrasound for folate-PEG liposomes, J. Drug Target. 20 (2012) 355–363.

[258] D. Omata, Y. Negishi, S. Hagiwara, S. Yamamura, Y. Endo-Takahashi, R. Suzuki, K. Maruyama, M. Nomizu, Y. Aramaki, Bubble liposomes and ultrasound promoted endosomal escape of TAT-PEG liposomes as gene delivery carriers, Mol. Pharmacol. 8 (2011) 2416–2423.

[259] M. Sugano, Y. Negishi, Y. Endo-Takahashi, N. Hamano, M. Usui, R. Suzuki, K. Maruyama, Y. Aramaki, M. Yamamoto, Gene delivery to periodontal tissue using bubble liposomes and ultrasound, J. Periodontal Res. 49 (2013) 398–404.

[260] E.T. Kisak, B. Coldren, C.A. Evans, C. Boyer, J.A. Zasadzinski, The vesosome – a multicompartment drug delivery vehicle, Curr. Med. Chem. 11 (2004) 199–219.

[261] P.S. Sheeran, P.A. Dayton, Phase-change contrast agents for imaging and therapy, Curr. Pharm. Des. 18 (2012) 2152–2165.

[262] P.S. Sheeran, S.H. Luois, L.B. Mullin, T.O. Matsunaga, P.A. Dayton, Design of ultrasonically-activatable nanoparticles using low boiling point perfluorocarbons, Biomaterials 33 (2012) 3262–3269.

[263] C.-Y. Lin, W.G. Pitt, Acoustic droplet vaporization in biology and medicine, BioMed Res. Int. 2013 (2013) 404361.

[264] R. Singh, G.A. Husseini, W.G. Pitt, Phase transitions of nanoemulsions using ultrasound: experimental measurements, Ultrason. Sonochem. 19 (2012) 1120–1125.

[265] W.G. Pitt, K.X. Perez, R.N. Singh, G.A. Husseini, D.R. Jack, Phase transitions of perfluorocarbon nanoemulsions induced with ultrasound: a mathematical model, Ultrason. Sonochem. 21 (2013) 879–891.

[266] M. Javadi, Novel Liposomes for Targeted Delivery of Drugs and Plasmids (Ph.D. thesis in Chemical Engineering), Brigham Young University, Provo, 2013.

[267] C.Y. Lin, M. Javadi, D.M. Belnap, J.R. Barrow, W.G. Pitt, Ultrasound sensitive eLiposomes containing doxorubicin for drug targeting therapy, Nanomedicine 10 (2013) 67–76.

[268] H.-Y. Lin, J.L. Thomas, PEG-lipids and oligo(ethylene glycol) surfactants enhance the ultrasonic permeabilizability of liposomes, Langmuir 19 (2003) 1098–1105.

[269] J.M. Escoffre, C. Mannaris, B. Geers, A. Novell, I. Lentacker, M. Averkiou, A. Bouakaz, Doxorubicin liposome-loaded microbubbles for contrast imaging and ultrasound-triggered drug delivery, IEEE Trans. Ultrason. Ferroelectr. Freq. Control 60 (2013) 78–87.

[270] S.K. Cool, B. Geers, S. Roels, S. Stremersch, K. Vanderperren, J.H. Saunders, S.C. De Smedt, J. Demeester, N.N. Sanders, Coupling of drug containing liposomes to microbubbles improves ultrasound triggered drug delivery in mice, J. Control. Release 172 (2013) 885–893.

[271] Y. Luan, T. Faez, E. Gelderblom, I. Skachkov, B. Geers, I. Lentacker, T. van der Steen, M. Versluis, N. de Jong, Acoustical properties of individual liposomeloaded microbubbles, Ultrasound Med. Biol. 38 (2012) 2174–2185.

[272] A.L. Klibanov, T.I. Shevchenko, B.I. Raju, R. Seip, C.T. Chin, Ultrasound-triggered release of materials entrapped in microbubble-liposome constructs: a tool for targeted drug delivery, J. Control. Release 148 (2010) 13–17.

[273] D. Yang, Y.H. Gao, K.B. Tan, Z.X. Zuo, W.X. Yang, X. Hua, P.J. Li, Y. Zhang, G. Wang, Inhibition of hepatic fibrosis with artificial microRNA using ultrasound and cationic liposome-bearing microbubbles, Gene Ther. 20 (2013) 1140–1148.

[274] E.C. Unger, Sonoporation and gene delivery with acoustically active carriers, Eur. J. Ultrasound 6 (1997) 1–2.

[275] M. de Smet, E. Heijman, S. Langereis, N.M. Hijnen, H. Grull, Magnetic resonance imaging of high intensity focused ultrasound mediated drug delivery from temperature-sensitive liposomes: an in vivo proof-of-concept study, J. Control. Release 150 (2011) 102–110.

[276] A. Partanen, P.S. Yarmolenko, A. Viitala, S. Appanaboyina, D. Haemmerich, A. Ranjan, G. Jacobs, D. Woods, J. Enholm, B.J. Wood, M.R. Dreher, Mild hyperthermia with magnetic resonance-guided high-intensity focused ultrasound for applications in drug delivery, Int. J. Hyperthermia 28 (2012) 320–336.

[277] C. Mannaris, E. Efthymiou, M.E. Meyre, M.A. Averkiou, In vitro localized release of thermosensitive liposomes with ultrasound-induced hyperthermia, Ultrasound Med. Biol. 39 (2013) 2011–2020.

[278] K. Komamura, R. Tatsumi, Y. Tsujita-Kuroda, T. Onoe, K. Matsumoto, T. Nakamura, J. Miyazaki, T. Horio, M. Sugimachi, Cellular injury of cardiomyocytes during hepatocyte growth factor gene transfection with ultrasound-triggered bubble liposome destruction, J. Drug Deliv. 2011 (2011) 453619.

[279] Y. Negishi, D. Omata, H. Iijima, N. Hamano, Y. Endo-Takahashi, M. Nomizu, Y. Aramaki, Preparation and characterization of laminin-derived peptide AG73coated liposomes as a selective gene delivery tool, Biol. Pharm. Bull. 33 (2010) 1766–1769.

[280] Y. Negishi, Y. Tsunoda, N. Hamano, D. Omata, Y. Endo-Takahashi, R. Suzuki, K. Maruyama, M. Nomizu, Y. Aramaki, Ultrasound-mediated gene delivery systems by AG73-modified bubble liposomes, Biopolymers 100 (2013) 402–407.

[281] S. Fujisawa, H. Arakawa, R. Suzuki, K. Maruyama, T. Kodama, M. Yasunaga, Y. Koga, Y. Matsumura, Optimum conditions of ultrasound-mediated destruction of bubble liposome for siRNA transfer in bladder cancer, Ther. Deliv. 1 (2010) 247–255.

[282] S. Dromi, V. Frenkel, A. Luk, B. Traughber, M. Angstadt, M. Bur, J. Poff, J. Xie, S.K. Libutti, K.C. Li, B.J. Wood, Pulsed-high intensity focused ultrasound and low temperature-sensitive liposomes for enhanced targeted drug delivery and antitumor effect, Clin. Cancer Res. 13 (2007) 2722–2727.

[283] S. Dromi, V. Frenkel, A. Luk, B. Traughber, M. Angstadt, M. Bur, J. Poff, J.W. Xie, S.K. Libutti, K.C.P. Li, B.J. Wood, Pulsed-high intensity focused ultrasound and low temperature sensitive liposomes for enhanced targeted drug delivery and antitumor effect, Clin. Cancer Res. 13 (2007) 2722–2727.

[284] A. Ranjan, G.C. Jacobs, D.L. Woods, A.H. Negussie, A. Partanen, P.S. Yarmolenko, C.E. Gacchina, K.V. Sharma, V. Frenkel, B.J. Wood, M.R. Dreher, Image-guided drug delivery with magnetic resonance guided high intensity focused ultrasound and temperature sensitive liposomes in

a rabbit Vx2 tumor model, J. Control. Release 158 (2012) 487–494.

[285] A.H. Negussie, P.S. Yarmolenko, A. Partanen, A. Ranjan, G. Jacobs, D. Woods, H. Bryant, D. Thomasson, M.W. Dewhirst, B.J. Wood, M.R. Dreher, Formulation and characterisation of magnetic resonance imageable thermally sensitive liposomes for use with magnetic resonance-guided high intensity focused ultrasound, Int. J. Hyperthermia 27 (2011) 140–155.

[286] R. Staruch, R. Chopra, K. Hynynen, Hyperthermia in bone generated with MR imaging-controlled focused ultrasound: control strategies and drug delivery, Radiology 263 (2012) 117–127.

[287] R.M. Staruch, M. Ganguly, I.F. Tannock, K. Hynynen, R. Chopra, Enhanced drug delivery in rabbit VX2 tumours using thermosensitive liposomes and MRIcontrolled focused ultrasound hyperthermia, Int. J. Hyperthermia 28 (2012) 776–787.

[288] R. Staruch, R. Chopra, K. Hynynen, Localised drug release using MRIcontrolled focused ultrasound hyperthermia, Int. J. Hyperthermia 27 (2011) 156–171.

[289] P.R. Patel, A. Luk, A. Durrani, S. Dromi, J. Cuesta, M. Angstadt, M.R. Dreher, B.J. Wood, V. Frenkel, In vitro and in vivo evaluations of increased effective beam width for heat deposition using a split focus high intensity ultrasound (HIFU) transducer, Int. J. Hyperthermia 24 (2008) 537–549.

[290] N. Hijnen, S. Langereis, H. Grull, Magnetic resonance guided high-intensity focused ultrasound for image-guided temperature-induced drug delivery, Adv. Drug Deliv. Rev. 72 (2014) 65–81.

[291] A. Kheirolomoom, C.Y. Lai, S.M. Tam, L.M. Mahakian, E.S. Ingham, K.D. Watson, K.W. Ferrara, Complete regression of local cancer using temperature-sensitive liposomes combined with ultrasound-mediated hyperthermia, J. Control. Release 172 (2013) 266–273.

[292] H. Kim, G.L. Britton, T. Peng, C.K. Holland, D.D. McPherson, S.L. Huang, Nitric oxide-loaded echogenic liposomes for treatment of vasospasm following subarachnoid hemorrhage, Int. J. Nanomed. 9 (2014) 155–165.

[293] S.L. Huang, P.H. Kee, H. Kim, M.R. Moody, S.M. Chrzanowski, R.C. Macdonald, D.D. McPherson, Nitric oxide-loaded echogenic liposomes for nitric oxide delivery and inhibition of intimal hyperplasia, J. Am. Coll. Cardiol. 54 (2009) 652–659.

[294] S.J. Huang, S.L. Sun, T.H. Feng, K.H. Sung, W.L. Lui, L.F. Wang, Folate-mediated chondroitin sulfate-Pluronic (R) 127 nanogels as a drug carrier, Eur. J. Pharm. Sci. 38 (2009) 64–73.

[295] H. Kim, P.H. Kee, Y. Rim, M.R. Moody, M.E. Klegerman, D. Vela, S.L. Huang, D.D. McPherson, S.T. Laing, Nitric oxide improves molecular imaging of inflammatory atheroma using targeted echogenic immunoliposomes, Atherosclerosis 231 (2013) 252–260.

[296] T. Peng, G.L. Britton, H. Kim, D. Cattano, J. Aronowski, J. Grotta, D.D. McPherson, S.L. Huang, Therapeutic time window and dose dependence of xenon delivered via echogenic liposomes for neuroprotection in stroke, CNS Neurosci. Ther. 19 (2013) 773–784.

[297] T. Kodama, A. Aoi, Y. Watanabe, S. Horie, M. Kodama, L. Li, R. Chen, N. Teramoto, H. Morikawa, S. Mori, M. Fukumoto, Evaluation of transfection efficiency in skeletal muscle using nano/microbubbles and ultrasound, Ultrasound Med. Biol. 36 (2010) 1196–1205.

[298] K. Hagisawa, T. Nishioka, R. Suzuki, K. Maruyama, B. Takase, M. Ishihara, A. Kurita, N. Yoshimoto, Y. Nishida, K. Iida, H. Luo, R.J. Siegel, Thrombustargeted perfluorocarbon-containing liposomal bubbles for enhancement of ultrasonic thrombolysis: in vitro and in vivo study, J. Thromb. Haemost. 11 (2013) 1565–1573.

[299] L. Mullin, L. Phillips, P. Dayton, Nanoparticle delivery enhancement with acoustically activated microbubbles, IEEE Trans. Ultrason. Ferroelectr. Freq. Control 60 (2013) 65–77.

[300] H. Mannell, J. Pircher, T. Rathel, K. Schilberg, K. Zimmermann, A. Pfeifer, O. Mykhaylyk, B. Gleich, U. Pohl, F. Krotz, Targeted endothelial gene delivery by ultrasonic destruction of magnetic microbubbles carrying lentiviral vectors, Pharm. Res. 29 (2012) 1282–1294.

[301] T. Rathel, H. Mannell, J. Pircher, B. Gleich, U. Pohl, F. Krotz, Magnetic stents retain nanoparticle-bound antirestenotic drugs transported by lipid microbubbles, Pharm. Res. 29 (2012) 1295–1307.

[302] D. Chen, J. Wu, An in vitro feasibility study of controlled drug release from encapsulated nanometer liposomes using high intensity focused ultrasound, Ultrasonics 50 (2010) 744–749.

[303] X.A. Chen, X.H. Wang, Y.S. Wang, L. Yang, J. Hu, W.J. Xiao, A. Fu, L.L. Cai, X. Li, X. Ye, Y.L. Liu, W.S. Wu, X.M. Shao, Y.Q. Mao, Y.Q. Wei, L.J. Chen, Improved tumor-targeting drug delivery and therapeutic efficacy by cationic liposome modified with truncated bFGF peptide, J. Control. Release 145 (2010) 17–25.

[304] H.L. Liu, P.Y. Chen, H.W. Yang, J.S. Wu, I.C. Tseng, Y.J. Ma, C.Y. Huang, H.C. Tsai, S.M. Chen, Y.J. Lu, M.Y. Hua, Y.H. Ma, T.C. Yen, K.C. Wei, In vivo MR quantification of superparamagnetic iron oxide nanoparticle leakage during low-frequency-ultrasound-induced blood-brain barrier opening in swine, J. Magn. Reson. Imaging 34 (2011) 1313–1324.

[305] Y. Chen, G.Z. Yu, D.H. Yu, M.H. Zhu, PKC alpha-induced drug resistance in pancreatic cancer cells is associated with transforming growth factor-beta 1, J. Exp. Clin. Cancer Res. 29 (2010).

[306] C.W. Burke, E.T. Alexander, K. Timbie, A.L. Kilbanov, R.J. Price, Ultrasoundactivated agents comprised of 5FU-bearing nanoparticles bonded to microbubbles inhibit solid tumor growth and improve survival, Mol. Ther. 22 (2014) 321–328.

[307] C.W. Burke, R.J. Price, Contrast ultrasound targeted treatment of gliomas in mice via drug-bearing nanoparticle delivery and microvascular ablation, J. Vis. Exp. (2010), http://dx.doi.org/10.3791/2145.

[308] S.J. Grainger, J.V. Serna, S. Sunny, Y. Zhou, C.X. Deng, M.E. El-Sayed, Pulsed ultrasound enhances nanoparticle penetration into breast cancer spheroids, Mol. Pharmacol. 7 (2010) 2006–2019.